Sudan University of Science & Technology
College of Graduate Studies

Synthesizing and A studying of Structural, Optical, and Electrical properties of pure Yttrium Barium Copper Oxide and Doped with Aluminum Oxide at Room Temperature.

تولیف ودراسة الخصائص التركيبية، البصرية والكهربية لأكسيد نحاس اليوتيريوم باريوم النقي والمشوب بأكسيد الآلمونيوم عند درجة حرارة الغرفة

A thesis submitted for the requirements of fulfillment of Ph.D. degree in Physics

Prepared by
Sarah Ezzedine Hamza Mudawi
M.Sc. Master of Science in physics (Solid State Physics) – June 2015 – SUST- Sudan
B.Sc. Bachelor of Science (HONOURS) in physics – Oct 2009 – SUST- Sudan

Supervisor
Dr. Mahmoud Hamid Mahmoud Hilo

April - 2021

بسم الله الرحمن الرحيم

قال تعالي

(... وقل رب زدني علما)

صدق الله العظيم

طه (114)

Acknowledgment:

At first my great thanks and love to Allah who helps me to conduct this research. I would like to pass my great thanks to my supervisor Dr: Mahmoud Hamid Mahmoud Hilo. Also my thanks and gratitude are extended to my family, friends and colleagues for their encouragement and support, which in turns make this study possible. Finally, Also thanks to any teachers helped me and my colleagues for their advice and in my PhD degree research.

Dedication:

To my father and my mother.

To my brothers and sisters.

To my husband and children.

To my friends and colleagues.

To all who helped me.

Abstract:

YBCO is a family of crystalline chemical compounds famous for displaying high-temperature superconductivity. The structural properties was studied by using X-ray powder diffraction (XRD), scanning electron microscope (SEM) and Fourier Transform Infrared (FT-IR). X-ray diffraction analysis showed that all samples have orthorhombic structures correspond to the high and low- phase with changing of the lattice parameters, and the crystal structure for pure $YBa_2Cu_3O_7$ is found to confirm the phase formation. Scanning Electron Microscope (SEM) pictures show uniform and homogeneous distribution, and the effect of the doping of aluminum oxide to the composite samples decreases the grains of the image of the distortion in the shape and structure. Fourier Transform Infrared spectrum showed that the $YBa_2Cu_3O_7$ is pure, and $YBa_2Cu_3O_7$ which doped with AL_2O_3 revealed perfectly. The optical properties for pure $YBa_2Cu_3O_7$ and $YBa_2Cu_3O_7$ which doped with AL_2O_3 was studied by using Ultraviolet-Visible Spectrophotometry (UV/VIS), the transmittance and absorbance spectra were recorded include the wavelength range of (200-800)nm, the results showed that Transmittance decreases with increasing in the wavelength between (200- 300) nm, and then remains constant with increasing wavelength, and absorbance increased with increasing wavelength between (200- 300) nm, and then remains constant with increasing the wavelength, and the Absorption Coefficient, refractive index and extinction coefficient were also calculated. The optical energy gap decreases with increase the doping with $YBa_2Cu_3O_7$ which doped with AL_2O_3, and also optical conductivity increases with elevated on absorbance. The electrical properties studied by using (I-V) measurements, also subjected our sample for (I-V)

characterization at different sample through four probe method and able to measure the critical current density (J_c) and found a decrement of critical current density with increment of doping, where electrical conductivity was calculated, the results also showed that The electrical conductivity for pure $YBa_2Cu_3O_7$ and $YBa_2Cu_3O_7$ doped with AL_2O_3 its increase with increased the doping concentration.

المستخلص:

يعتبر YBCO من عائلة المركبات الكيميائية البلورية والتي تشتهر بعرض الموصلية الفائقة في درجات الحرارة العالية حيث تم تحضير YBCO اليتريوم باريوم نحاس النقي والمطعم باكسيد الألومنيوم. تمت دراسة التركيب البلوري باستخدام حيود الاشعة السينية **(XRD)** والمجهر الإلكتروني الماسح**SEM** وتحويل فوريية الاشعه تحت الحمراء **(FT-IR)** . واظهر تحليل حيود الأشعة السينية أن جميع العينات لها تركيبات تتوافق مع جميع الاطوار العليا والمنخفضة مع تغيرات معاملات الشبيكة،وتم العثور علي التركيب البلوري ل YBCO النقي لتاكيد تكوين الطور.وقد اظهرت صور المجهر الإلكتروني الماسح توزيعآ موحدا ومتجانسا، ويكون تاثير التطعيم من أكسيد الالومنيوم علي العينات المركبة في حجم الحبيبات حيث تظهر صغيرة وتكون الصورة متغيرة في الشكل والبنية. اظهر طيف الأشعة تحت الحمراء لتحويل فورييه ان YBCO نقي، وأن YBCO الذي تم تطعيمه باستخدام أكسيد الالومنيوم قد كشف تماما. تمت دراسة الخواص البصرية YBCO النقي والمطعم بأكسيد الالومنيوم باستخدام مقياس الطيف الضوئي المرئي فوق البنفسجي(UV/VIS)، وتم تسجيل اطياف النفاذية والامتصاصية وتشمل مدي الطول الموجي (٢٠٠-٨٠٠) نانو متر، واظهرت النتائج ان النفاذية تتناقص مع زيادة الطول الموجي في المدي بين (٢٠٠-٣٠٠) نانومتر ثم يظل ثابتا مع زيادة الطول الموجي ، ويزداد الامتصاص مع زيارة الطول الموجي(٢٠٠-٣٠٠) نانومتر ثم يظل ثابتا مع زيادة الطول الموجي ومعامل الامتصاص ، كما تم حساب معامل الانكسار ومعامل الخمول. تقل فجوة الطاقة الضوئية عندما نزيد نسبة التطعيم بأكسيد الألومنيوم،وكذلك تزداد الموصلية الضوئية بزيادة الامتصاصية. تمت دراسة الخواص الكهربائية باستخدام قياسات الجهد والتيار، وتم ذلك بتعريض العينة لخصائص الجهد والتيار من خلال طريقة أربعة مجسات وتم قياس كثافة التيار الحرجة (J_c) ووجد ان كثافة التيار الحرج تقل عند زيادة نسبة التشويب ،حيث تم حساب التوصيلية الكهربائية، واظهرت النتائج ايضا ان التوصلية الكهربائية لكل من النقي والمشوب بأكسيد الألومنيوم تزداد بزيادة تركيز التطعيم.

Contents:

Table and Figures:

List of Abbreviations:

Sample	Abbreviation
T_c	Critical temperature
XRD	X-ray diffraction
UV-Vis	Ultraviolet-visible Spectroscopy
BEC	Bose- Einstein–condition
BCS	Bardeen-cooper-Schrieffer
YBCO	Yttrium Barium Copper Oxide
NT	Neel Temperature
SEM	Scanning Electron Microscope
HDC	Continuous Magnetic Field

CHAPTER ONE

1.0 Introduction to Superconductivity

1.1 The Solid State

Matter is something that has mass and occupies space .It is characterized by a set of properties such as shape, size, mass, melting point, boiling point, color, texture, reactivity, etc. Based on size shape, volume and rigidity, matter is classified into three categories solid, liquid and gaseous [1]. There are some simplifying features of solids which allow considerable insight into their nature. The solids have definite shape and volume and are rigid Therefore solids are characterized by rigidity incompressibility and mechanical strength. These facts indicate that the atoms ions or molecules, which make up the solids, are very closely packed [2]. They are held together by strong forces of attraction and are not free to move at random. The solids are, therefore, the outcome of well-ordered arrangement of building units. A good understanding of nature and properties of solids will provide a wide range of tailor-made materials with specific properties having uses in the development of science and technology. Much of our recent progress is no doubt due to the advances we have made in solid-state physics [3].

1.2 Types of Solids:

From the state of aggregation the solids are grouped into two categories: amorphous and crystalline.

1.2.1 Crystalline Solid:

The Solids whose constituents are arranged in a regular geometrical pattern

over the entire lattice be knows as the crystalline Solids. This is proved to be so by X –ray diffraction study .Due to the orderly arranged atoms, ions or molecules the crystalline Solids exhibit different elements of symmetry and accordingly belong to either of the crystal systems. [4]

1.2.2 Metallic Crystals:

The crystalline Solids having positively charged metal ions in the lattice points, surrounded by a sea of mobile electrons are known as metallic crystals. For example: Copper, Silver, gold, sodium, potassium, iron, cobalt, nickel, etc. Here the binding force is the electrical attraction between positively charged metal ions and negatively charged sea of mobile electrons. On account of this fact many typical features characterize the metals. They may be soft or hard sufficiently tough, with moderate to very high melting points, good conductors of heat and electricity. These are malleable, ductile and elastic with high tensile strength; exhibit good Ouster on fresh cut etc. (Exception – mercury). In the present chapter our aim is to discuss crystalline Solids such as metals semiconductors and super-conductors. [4]

1.2.3 Metals:

The most numerous of all the elements are the metallic elements. All the elements in the s, d and f blocks are metals: aluminum, gallium, indium, thallium, tin, lead and bismuth of the p-block are considered to be metals. Further, germanium and polonium are also sometimes taken to be metallic elements. Thus the metals constitute about eighty percent of the element in the periodic Table. It appears that the element with too little electrons in the valence shell but with too many orbitals behave as metals. No doubt, metals are marvels among elements. The marvelous characteristics such as luster, conductivity, malleability, ductility, etc of metals have been attributed to the

metallic bond. Metals mean such to modern man. Every amenity of modern civilization depends heavily on metals. In fact there is no moment when man is not in contact with metallic objects directly or indirectly. In other words the distinctive applications of metals are due to the strange nature of forces that exist within the metals .Hence to understand metals it is wise to make an attempt only through their special features[5].

1.3 Energy Band Theory:

According to Bohr's theory, every shell of an atom contains a discrete amount of energy at different levels. Energy band theory explains the interaction of electrons between the outermost shell and the innermost shell. Based on the energy band theory, there are three different energy bands [6]:

- Valence band.
- Forbidden energy gap.
- Conduction band.

1.3.1 Valence Band:

The electrons in the outermost shell are known as valence electrons. These valence electrons contain a series of energy levels and form an energy band known as valence band. The valence band has the highest occupied energy.

1.2.2 Conduction Band:

The valence electrons are not tightly held to the nucleus due to which a few of these valence electrons leave the outermost orbit even at room temperature and become free electrons. The free electrons conduct current in conductors and are therefore known as conduction electrons. The conduction band is one that contains conduction electrons and has the lowest occupied energy levels [7].

1.3.3 Forbidden Energy Gap:

The gap between the valence band and the conduction band is referred to as forbidden gap. As the name suggests, the forbidden gap doesn't have any energy and no electrons stay in this band. If the forbidden energy gap is greater, then the valence band electrons are tightly bound or firmly attached to the nucleus. We require some amount of external energy that is equal to the forbidden energy gap [8].

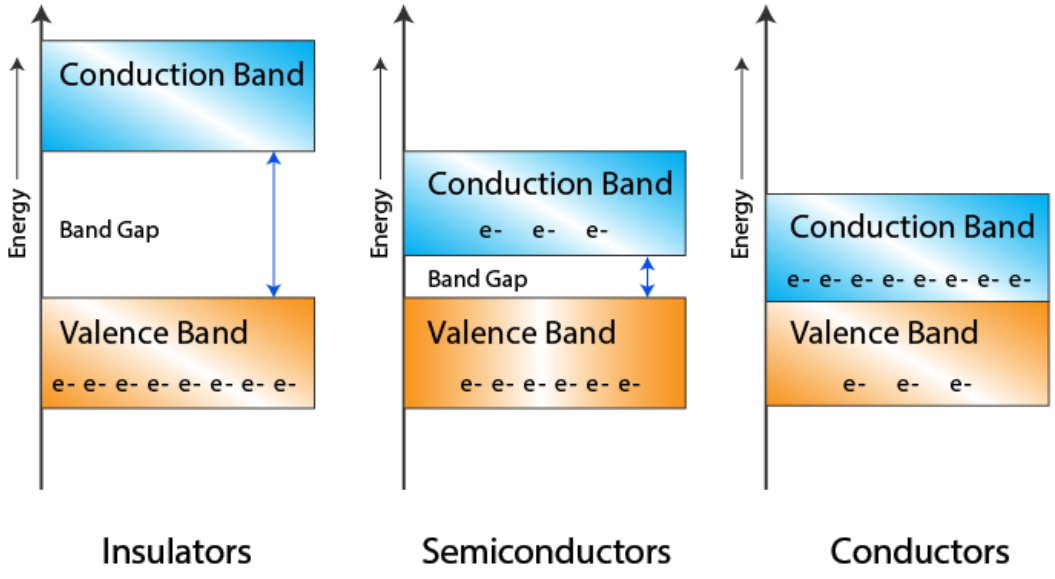

Fig (1.1) Energy band diagram

1.4 Classification of Energy Bands:

1.4.1 Conductors:

Gold, Aluminum, Silver, Copper, all these metals allow an electric current to flow through them. There is no forbidden gap between the valence band and conduction band which results in the overlapping of both the bands. The number of free electrons available at room temperature is large [9].

1.4.2 Insulators:

Glass and wood are examples of the insulator. These substances do not allow electricity to pass through them. They have high resistivity and very low conductivity. The energy gap in the insulator is very high up to 7eV. The material cannot conduct because the movement of the electrons from the valence band to the conduction band is not possible [9].

1.4.3 Semiconductors:

Germanium and Silicon are the most preferable material whose electrical properties lie in between semiconductors and insulators. The energy band diagram of semiconductor is shown where the conduction band is empty and the valence band is completely filled but the forbidden gap between the two bands is very small that is about 1eV. For Germanium, the forbidden gap is 0.72eV and for Silicon, it is 1.1eV. Thus, semiconductor requires small conductivity [10].

1.5 Superconductor:

Metals are good conductors of electricity and their conductivity increases as the temperature decreases. In 1911 the Dutch scientist Kamerlingh Onnes discovered the phenomenon of superconductivity when he was studying electrical properties of materials near absolute zero. A superconductor has zero or almost zero electrical resistance. It can therefore carry an electric current without losing energy. In other words the current can flow forever. It was proved that mercury is a superconductor below 4.2 K – (the critical temperature (T_c) at which the superconducting state is formed [2].

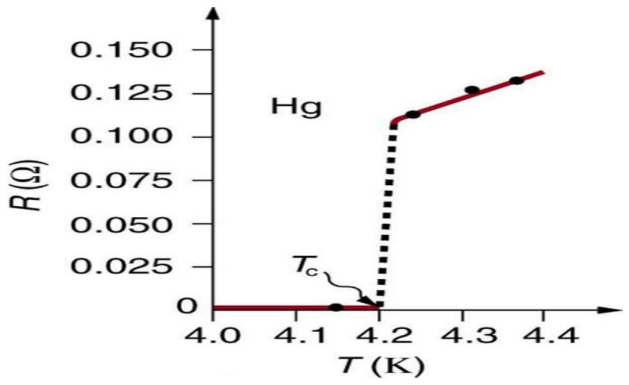

Fig (1.2) Resistance – Temperature variation of Hg

1.5.1 Properties of superconductor:

Materials having high normal resistivity exhibit superconductivity. Superconductivity is exhibited by metallic elements in which the number of valence electrons lies between 2 and 8. Transition temperature T_C varies from sample to sample. The transition range for chemically pure and structurally perfect specimen is very small but impure and structurally imperfect is broad. Transition metals having odd number of valence electrons are better than those having even number of valence electrons as regards superconductivity is concerned. Elements with small atomic volume and atomic mass are better superconductors. T_c varies linearly with Z^2, where Z is the number of valence electrons. Ferromagnetic and antiferromagnetic materials do not show superconductivity. In a superconductivity ring, current persists for a long time.

1.5.2 Type I and Type II superconductors:

On the basis of diamagnetic response of material, superconductors are of two types, type I and type II. Type I superconductors are those for which Meissner effect is complete, i.e., perfect diamagnetism. Below critical

magnetic field (H_c), if the magnetic field H gradually increased from its initial value the magnetization M increases at H = H_c, the diamagnetism abruptly disappear. In type II superconductor when the magnetic field is increased from H = 0 to H = H_{c1}, the material behaves as pure superconductor and line of flux rejected. If h increased beyond H_{c1} the material is in mixed state up to H_{c2} and flux begins penetrating, Meissner effect is incomplete in this region [6].

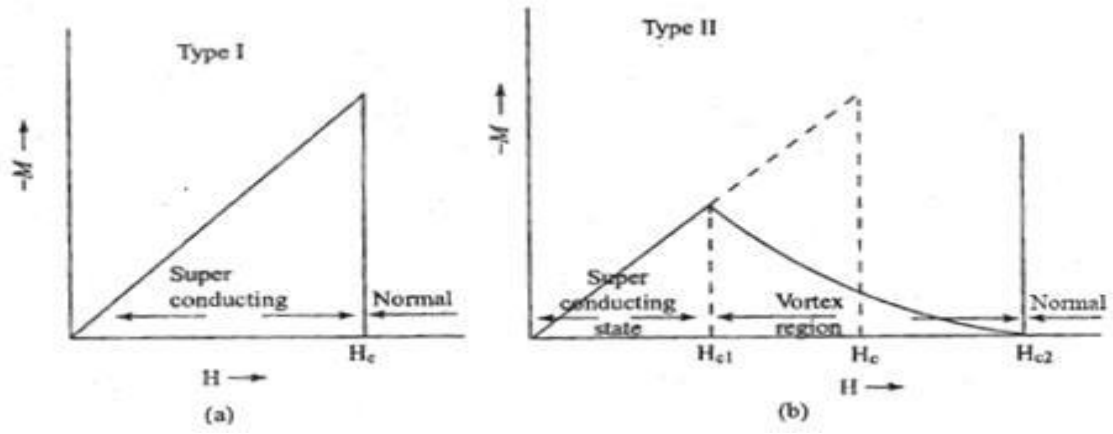

Fig (1.3) Type I and Type II superconductor

1.5.3 Theories of Low Temperature Superconductor:

During the first half of the century after the discovery of superconductivity the problem of fluctuation smearing of the superconducting transition was not even considered. In bulk samples of traditional superconductors the critical temperature Tc sharply divides the superconducting and the normal phases. It is worth mentioning that such behavior of the physical characteristics of superconductors is in perfect agreement both with the Landau- Ginzburg- Landau (GL) phenomenological theory (1950) and the

BCS microscopic theory of superconductivity (1957)[6].

1.5.3.1 The London theory:

Electron conduction in the normal state of a metal is described by Ohm's law j= σ × E . We modifies this to describe and the Meissner effect in the superconducting state. We assume that in the superconducting state the current density is directly proportional to the vector potential A of the local magnetic field. Here, ($B = \nabla \times A$) The constant of proportionality is ($-\frac{1}{\mu o}\lambda^{0}{}_{L}$) [24].

$j = (-\frac{1}{\mu o}\lambda^{0}{}_{L})$ A……(1.1)

Here, λ_L is a constant with the dimensions of length.

This is the London equation.

Taking the curl of both sides, we get

$\nabla \times J = (-\frac{1}{\mu o}\lambda^{0}{}_{L})$ B ……(1.2)

Now, consider the Maxwell equation

$\nabla \times J = \mu \circ j$ …….(1.3)

$\nabla \times \nabla \times B = \mu \circ \nabla \times j$ ……(1,4)

Now, $\nabla \times \nabla \times B = grad\ div\ B - \nabla^2 B$

$\nabla \times \nabla \times B = -\nabla^2$ B (div B = 0)

$-\nabla^2$ B = μ ∘ ∇ × j − ∇^2 B = μ ∘ ∇× j ….....(1.5)

$-\nabla^2$ B = $-[\frac{n_s\ e^2\ \mu\circ}{m}]$ B=$-\frac{B}{\lambda 2}$ ……...(1.6)

$$\lambda^2 = (\frac{m}{n_s e^2\ \mu_\circ}) \quad \text{.....(1.7)}$$

Where λ: is the London penetration depth (this term relates to how deeply a magnetic field will penetrate the surface of a superconductor). Combining this definition with the **GC** form for the density of superconducting electrons results in a temperature dependent penetration depth,

$$\lambda(T) = \frac{\lambda(0)}{\sqrt{1+t^4}} \quad \text{.....(1.8)}$$

Although Eq (1.8) has no microscopic justification, at low temperatures it takes the form , $\lambda(T) \approx \lambda(0)\{\left(1 + \frac{t^4}{2}\right) + 0(t^8)\}$ which is nearly indistinguishable from the exponential behavior $\lambda(T) \approx T^{-1/2} e^{(-\frac{\Delta}{T})}$ predicted by BCS theory[25].

$$\lambda(T) = \lambda(0)[1 - (\frac{T}{T_c})^4]^{-1/2} \quad \text{.....(1.9)}$$

where λ(0)is the penetration depth at T=0K. Fig.(1.4)shows the variation of penetration depth with temperature[10].

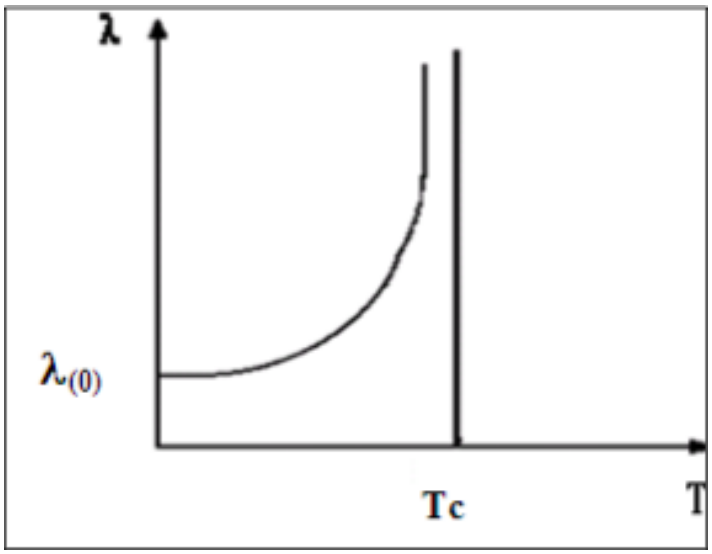

Fig (1.4) penetration depth(λ) changes with the temperature

1.5.3.2 Ginzburg-Landau theory:

Ginzburg-Landau theory macroscopically describes the behavior of superconductors, including quantum effects. It assumes a second order phase transition, which is correct for ZFC. It also assumes that the conduction electrons in a superconductor behave in a coherent manner, allowing them to be described by a single wave function with a possible phase difference [11].

$$\psi(r) = |\psi(r)|e^{i\varphi} \quad \text{.....(1.10)}$$

We must now define two characteristic lengths for a superconductor. The first is the coherence length(ζ) .One victory of Ginzburg-Landau theory is the prediction of type-II superconductivity. Defining ($\kappa = \lambda / \xi$), we can make a statement about the sign of the interface energy σns[11] . The interface between two such domains is shown in Fig. (1.5). The ratio of penetration depth (λL) to coherence length (ζ) is known as Ginzburg Landau parameter (k) this parameter leads to a classification of superconductors into two types (Type I and Type II) as shown in Fig. (1.5).

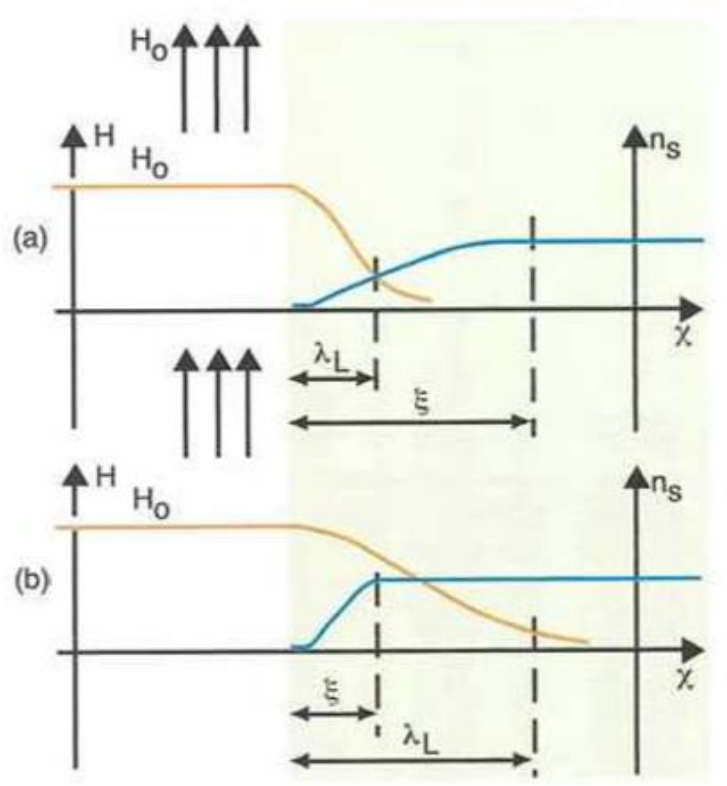

Fig (1.5) The boundary between superconducting (green) and normal (white) phases. The dependence of the magnetic field strength H and the number of superconducting electrons on the distance across the boundary are illustrated in (a) a type I superconductor and (b) a type I1 superconductor

1.5.3.3 BCS (Bardeen-Cooper-Schrieffer) theory of superconductor:

To designate the superconducting occurrences Bardeen, Cooper, and Schrieffer known as BCS theory suggested a microscopic theory. In superconducting state the electrons form bound pair called Cooper. The Cooper pair basically formed due to the electron-electron interaction with an exchange of phonon. If we consider that the conduction electrons inside the Fermi sphere and the two electrons lying just inside the Fermi surface and they form pair of electrons. The Fermi surface electrons travels faster in the

lattice. The positive core is attracted from the electrons. Due to the screening effect of the positive charges, the electronic charges are decreases. In this region electrons are in stable position takes enough positive charges in normal state that the lattice becomes distorted. During the formation of Cooper pair first electron release a phonon, which is absorbed by the other electron [8]. When the temperature is less than the transition temperature, the lattice-electron interaction is greater than electron-electron in that temperature range. The Cooper pair travels easily in the lattice with constant momentum and without any exchange of energy to the lattice meanwhile the pair gathering contains high degree of association in their motion [8].

1.5.4 Application of superconductivity:

- Switching devices:- The transition from superconducting state to normal state when the applied magnetic field be larger than the transition field and is opposite when the field is removed. We have use this property to make switching element cryotron.

- Electric generators:- The superconductor coil is winding in an top of greater magnetic field to create electric powers. This generators at very low voltage (450 V) could be generate very high powers (nearly 2500 kV). From that generator we can save the power and the size and weight of the generator is very low.

- Generation of magnetic field:- The application of superconducting materials that can be generates high magnetic field (nearly 50 T). The power require to such a high magnetic field is only 10 kW but in general to generate such a high magnetic

field require 3 MW power.

- Low loss transmission line and transformers:- The resistance of the superconductor nearly zero so in superconducting wire power loss is very small. In transformer if the primary and secondary winding by a superconducting wire so that heat will be minimum and power loss will be very less.

- Magnetic levitation:- The superconducting materials exhibits diamagnetic behavior that rejects all the magnetic field lines and this is used in magnetic levitation. The magnetic levitation can be utilized in high-speed transportation.

- Magnetic resonance imaging (MRI):- MRI is depend on the property of superconductivity and in a magnetic field there is a special type of behavior of atoms. In human body there are large number of hydrogen atoms and other elements. The nuclei of atoms tend to align like a compass needle in the attendance of magnetic field [12].

1.6 Previous studies:

Kenji IIMURA[3] etal .. ,Received January 19, 2017; Accepted June 6, 2017], Preparation of yttrium barium copper oxide superconductive fibers via electrospinning through a lactic-acid gel route, A new synthetic route to YBCO superconductive fibers using electrospinning together with the polymerizable complex method was successfully developed. The tactile, as-spun fibers were wool-like, and the thickness of the fibers was 57 ¯m; consequently, the fibers exhibited sufficient flexibility to be fabricated into arbitrary shapes. The results of TG/DTA measurements revealed that the

mass fraction of organic substance was reduced to 55%, which is remarkably low compared with the corresponding fraction in fibers prepared by the conventional polymerizable complex method. Although the fibers shrunk and exhibited brittle tactility because of the decomposition of organic substances during the heat treatment, the fibers nonetheless predominantly maintained their fibrous form because of their reduced content of organic matter. SEM observations revealed the growth of metal oxide grains during sintering. The powder XRD pattern of the annealed fibers were consistent with the pattern of YBa2Cu3O7¤. The magnetic property measurements using a SQUID magnetometer revealed that the ground samples exhibited a Tc of 91 K.

A. Arlina1 etal.., 2016 UMK Publisher. All rights reserved., Synthesis and Effect of Al2O3 Added in Yttrium Barium Copper Oxide YBa2Cu3Oδ by Solid State Reaction Method, The YBCO pure powder was successfully synthesize and confirmed its phase and quality of the samples. On top of that, Al2O3 nanoparticles addition were successfully introduced and well distributed into YBCO superconductor through solid state reaction. In this paper a systematic study on the addition of Al2O3 nanoparticles with different weight percentage to YBa2Cu3O7 was the orthorhombic structure and the is no structure change in the superconducting YBCO compound due to Al addition, a few additional peaks located at 2θ = 29.82° and 30.50°, compared to pure YBCO.

- **N. Y. Erwana1 etal…, 11 January 2018; Published:** 11 May 2018, Preparation and Characterization of Yttrium Barium Copper Oxide (YBCO) Superconductor with Addition of Cobalt Oxide (CO3O4), n Superconducting ceramic material of YBCO with a ratio of 1:2:3

compositions were analyzed. The critical temperature (T_c) measurement shows that the addition of cobalt oxide to YBCO superconductor was increased from 58 K of x= 0.00 wt% to 87 K of x= 0.02 wt%. The XRD of YBCO samples proved that the sintered material consist of Y123, single phase. All samples showed the structure of YBCO orthorhombic structure. SEM characterization showed that the grain size increased as increasing of the weight percentage of cobalt oxide.

Dr. Youwen Xu etal…, on May 7, 2014, Crystal Structure and Superconductivity of YBa2Cu3O7-x, on, A set of YBa2Cu3O7-x samples were made by quenching fully-oxygenated samples after high-temperature annealing. The oxygen contents were 6:79; 6:65; 6:54; 6:46; and 6:33. The lattice parameters a and c were observed to monotonically increase while b nearly monotonically decreases with decreasing oxygen content. All samples had orthorhombic symmetry; hence no orthorhombic to tetragonal phase transition was observed. The lattice parameters of our samples are consistently smaller than those reported in the literature. Magnetization measurements indicated that Tc as well as superconducting volume fraction decreased as oxygen content decreased. Most Tc values were consistent with the literature for samples with similar oxygen content. Similar to results reported in the literature, a plateau in Tc values between samples with oxygen contents 6:50 . 7 - x . 6:75 was observed, possibly due to the ordering of the oxygen atoms at the copper-oxygen chain sites. Our results for crystal structure and superconductivity in YBa2Cu3O7-x are consistent with the model describing the decrease in Tc as a result of oxygen being removed from the copperoxygen chain sites. The discrepancies in lattice parameters for samples in this study with those reported in the literature are likely caused by the original sample not being fully oxyenated, the actual

oxygen content may be approximately 6.95 instead of 7.00. To ensure samples are fully oxygenated, synthesis of YBa2Cu3O7 samples by the procedure in this study should be limited to a batch size less than 10 g. Other methods of creating oxygen-deficient samples should be considered for future studies on the normal state magnetization of YBa2Cu3O7-x. Instead of annealing YBa2Cu3O7 in air to prepare oxygen-deficient samples, annealing could be done at a constant temperature with controlled argon-oxygen mixtures.

S. Alikhanzadeh-Arania etal…, Published online 1/1/2012, Synthesis and characterization of high-temperature ceramic YBCO nanostructures prepared from a novel precursor, In conclusion, we have demonstrated the synthesis of YBCO nanostructures from the ([tris(2-hydroxyacetophenato) triaqua (III)], [Y(HAP)3(H2O)3]) as new precursor via a solid state process at different temperature for 12 h. It was found that by using the coordination compositions as new raw materials, it can be possible to achieve the superconducting phase at lower calcination temperature (870 ºC). Moreover, there was no need to use any surfactant or protective agent for controlling size of products due to steric hindrance of methyl groups around metal ion. From the results of XRD, FT-IR and TEM, the as-prepared sample shows good morphologies corresponding to rod-like nanostructures with length of about 320–350 nm and diameters about 60–90 nm.

ZHAO GaoYang1 etal…, published online April 30, 2013, Fabrication of YBCO superconducting microarray by sol-gel process using photosensitive metal chelates, YBCO/BzAcH sol can be synthesized using yttrium acetate, barium acetate, and copper acetate as the starting materials, benzalacetone (BzAcH) as chemical modifier, and methanol (MEOH) as solvent. BzAcH, as a chemical modifier, can react with the metal ions to form the

photosensitive metal chelate rings which have good chemical stability in the YBCO/BzAcH sol. The photosensitive YBCO/BzAcH gel film can be patterned to form the fine-patterns and microarray with a pitch of 5 μm by the UV light irradiating through a mask. The YBCO fine-patterns exhibit good c-oriented epitaxy and superconductivity after a proper heat-treatment.

M. Lyatti etal.. , Experimental evidence for hotspot and phase-slip mechanisms of voltage switching in ultra-thin YBa2Cu3O7-x nan, We have observed two types of current-induced voltage switching in the IV curves of ultra-thin YBCO nanowires. Voltage switching in the flux-flow IV curves occurs due to the hotspot-assisted suppression of the edge barrier by the transport current. Here, the bias current values at which hotspot-assisted voltage switching occurs is in good quantitative agreement with the predictions of the Aslamazov-Larkin model for wide superconducting bridges. The direct voltage switching of nanowires with small cross-sections (Wd ≤ 1500 nm2) is attributed to the appearance of phase-slip lines in the YBCO nanowire.

Ahmed M. etal.., Structural, electrical, magnetic, and flux pinning properties of YBCO/Ni superconducting composites: analyses and possible explanations, Unexpected improvements of SC state properties of some YBCO + xNi (where x ≤ 2.5 wt.%) has been suggested as due to high JT distortions. These samples are found to have YBCO crystallites with high c/a ratios. We have proposed that these composites have high value of ΔA and high in-plane hopping integrals on average. YBCO-crystallites with low level of Ni additives, in-plane Ni2+ barely perturbs the short-range AF correlations that are supposed to have effective role in the pairing processes of the ZR singlets. Further addition of Ni2+ leads to an unavoidable substitution in the Cu sites which gives rise to localization of in-plane hole

carriers in vicinity of Ni2+ and in turn scattering of moving ZR singlets-pairs. These result in the degraded state of superconductivity for composites with high level of Ni wt.%.

\

CHAPTER TWO

2.0 Superconducting system

2.1 Introduction

Kamerlingh Onnes discovered the phenomenon of superconductivity in 1911, in metallic mercury below 4 K (−269.15 °C). Ever since, researchers have attempted to observe superconductivity at increasing temperatures with the goal of finding room-temperature superconductor. By the late 1970s, superconductivity was observed in several metallic compounds (in particular Nb- based, such as NbTi, Nb_3Sn, and Nb_3Ge) at temperatures that were much higher than those for elemental metals and which could even exceed 20 K (−253.2 °C)[13]. In 1986, J. Georg Bednorz and K. Alex Müller, working at the IBM research lab near Zurich, Switzerland were exploring a new class of ceramics for superconductivity. Bednorz encountered a barium-doped compound of lanthanum and copper oxide whose resistance dropped to zero at a temperature around 35 K (−238.2 °C). Their results were soon confirmed by many groups, notably Paul Chu at the University of Houston and Shoji Tanaka at the University of Tokyo. Shortly after, P. W. Anderson, at Princeton University came up with the first theoretical description of these materials, using the resonating valence bond theory, but a full understanding of these materials is still developing today. These superconductors are now known to possess a d-wave pair symmetry The first proposal that high-temperature cuprate superconductivity involves d-wave pairing was made in 1987 by Bickers, Scalapino and Scalettar followed by three subsequent theories in 1988 by Inui,

Doniach, Hirschfeld and Ruckenstein, using spin-fluctuation theory, and by Gros, Poilblanc, Rice and Zhang, and by Kotliar and Liu identifying d-wave pairing as a natural consequence of the RVB theory. The confirmation of the d-wave nature of the cuprate superconductors was made by a variety of experiments, including the direct observation of the d- wave nodes in the excitation spectrum through Angle Resolved Photoemission Spectroscopy, the observation of a half- integer flux in tunneling experiments, and indirectly from the temperature dependence of the penetration depth, specific heat and thermal conductivity Until 2015 the superconductor with the highest transition temperature that had been confirmed by multiple independent research groups (a prerequisite to being called a discovery, verified by peer review) was mercury barium calcium copper oxide ($HgBa_2Ca_2Cu_3O_8$) at around 133 K. After more than twenty years of intensive research, the origin of high-temperature superconductivity is still not clear, but it seems that instead of electron-phonon attraction mechanisms, as in conventional superconductivity, one is dealing with genuine electronic mechanisms (e.g. by antiferromagnetic correlations), and instead of conventional, purely s-wave pairing, more exotic pairing symmetries are thought to be involved (d-wave in the case of the cuprates, primarily extended s- wave, but occasionally d-wave, in the case of the iron-based superconductors). In 2014, evidence showing that fractional particles can happen in quasi two- dimensional magnetic materials, was found by EPFL scientists lending support for Anderson's theory of high- temperature superconductivity [8].

2.2 Crystal structures of high temperature superconductors:

The structure of high-Tc copper oxide or cuprate superconductors are often closely related to perovskite structure, and thestructure of these compounds has been described as a distorted, oxygen deficient multi-layered perovskite structure. One of the properties of the crystal structure of oxide superconductors is an alternating multi-layer of CuO_2 planes with superconductivity taking place between these layers. The more layers of CuO_2, the higher Tc. This structure causes a large anisotropy in normal conducting and superconducting properties, since electrical currents are carried by holes induced in the oxygen sites of the CuO_2 sheets. The electrical conduction is highly anisotropic, with a much higher conductivity parallel to the CuO_2 plane than in the perpendicular direction. Generally, critical temperatures depend on the chemical compositions, cations substitutions and oxygen content. They can be classified as superstripes; i.e., particular realizations of superlattices at atomic limit made of superconducting atomic layers, wires, dots separated by spacer layers, that gives multiband and multigap superconductivity [12].

2.2.1 Theories of High Temperature Superconductor:

The discovery of superconductivity in ceramic marked the beginning of high temperature superconductor (HTSc). Many theoretical models have been proposed to explain the pairing mechanisms in HTS [11].

2.2.1.1 Excitons and Plasmons Model:

Allender etal proposed a metal into such intimate contact with analogue to a polarizable narrow gap semiconductor that the metallic electrons would be able to interact strongly with interband excitations of the semiconductor[11]. Pairing would then occur by the exchange of these

virtual excitations. The Plasmon mechanism, looks like the exciton mechanism. Eliashbreg assumes that electronic polarization serves only to cancel part of the direct coulomb repulsion, and that only phonon polarization is sufficiently strong and retarded to contribute to pair binding. Thus, a reasonable question is whether, in the absence of phonons, the other polarization mechanisms can cause superconductivity [11].

2.2.1.2 Interlayer Coupling Model:

In this model, the superconductivity occurs in the two-dimensional $Cu\text{-}O_2$ layers, and interlayer tunneling is essential because the coherence length normal to the $Cu\text{-}O_2$ layer is so short [13]. So the supercurrent could then flow between $Cu\text{-}O_2$ layers by taking the advantage of the metallic states on the intervening layers, essentially hopping from copper-oxygen layer to another copper-oxygen layer by tunneling through the metallic interlayer[14,11].

2.2.1.3 Isotope Model:

The important point to be noted is that an isotope effect strongly indicates that phonons are involved in the pairing and that the lack of an isotope effect cannot be interpreted as a conclusive evidence of the absence of phonon mediated pairing [14,11].

2.2.1.4 Oxygen Defect Model:

This model depends on the fact that the structural analysis of the unit cell shows that there are oxygen defects (vacancies) in the $Cu\text{-}O_2$ layers, and suggests that the special structure of the oxygen defects together with the electronic filling of Copper pairs in particular are combined to enhance the pairing interaction significantly in HTS

materials [14]. The vacancies are assumed to be randomly distributed in the copper oxide planes. One-electron energetically attract electrons to the pairs of copper ions next to vacancies. Electrons at these sites have an enhanced probability to be found between the two ions with singlet spin correlation. Similarly, there are many reported experimental phenomena including spin glass-like behavior emphasize the dependence of the superconducting properties on the oxygen content of the oxide and this leads to shortening of positron lifetimes in the superconductors.

2.3 Properties of high temperature superconductor:

- In general oxide high temperature superconductor the conduction charge carrier is holes rather than electron.

- The magnetism and superconductivity are hardly found in earth compound and in the process of superconductivity the earth ions does not contribute.

1. In superconducting state of low temperature the specific heat is

$$C = aT_2 + bT_3 + Ct. \quad \ldots\ldots\ldots\ldots (2.1)$$

The first term is due to the Schottky like irregularity, the second term due to lattice of Debye contribution and the third term because of conduction of free electron.

- All the high temperature superconductor are type II superconductor, highly anisotropic with Hc1 and Hc2.

When the pressure increases in high temperature superconductors the critical

- temperature will be increases, however reverse effect is found in predictable superconductors.

- In high temperature superconductors does not present the isotopic effect.

- Temperature dependent and highly anisotropic conduction properties in normal state.

- The Josephson tunneling in high temperature superconductors.

2.4 YBCO superconductor:

YBCO is a high temperature superconductor whose transition temperature starts at 93 K and zero resistance below the onset temperature of Tc. YBCO is a type II superconductor in that it has both Meissonier effect and intermediate state. However, there are certain changes in the way the intermediate state operates. In YBCO the cooper pairs as being the pairing of holes rather than electrons. Using holes as a charge carrier means that the charges that move are positive rather than negative. Holes in the curate superconductors come from the Cu2+ and Cu3+ states that are present. The number of holes copper oxide conduction planes is prejudiced by the ratio of these two states. This ratio can be altered by the quantity of oxygen present in the planes. The superconductive state is be contingent on the awareness is met. This is why changing the oxygen gratified in YBCO differs the critical temperature since this is done the concentration of holes is affected [15].

2.5 Structure of YBCO:

The structure of YBCO acts a significant role in superconductivity. YBCO has a layered structure containing copper oxygen planes with Yttrium and Barium

atoms in the crystal structure in addition. The subsequent crystal structure is related to a pervoskite with a unit cell involving of fixed cube of BaCuO3 and YCuO3. In figure shows the structure and the chemical arrangement of the planes formed [15]. One significant entity to note that is the two unlike planes of copper and oxygen. The planes below and above the Yttrium atoms have two oxygen atom per copper where Yttrium has planes close it with one copper per oxygen. These planes that are one to one are said to be oxygen lacking since when related to a whole perovskite structure there are two oxygen atoms omitted. The superconducting of the system appears to rise from these copper oxide layer since they are mutual to the copper oxide superconductors. The two planes detached by an atoms of Yttrium, a distance of 3.2 A. The current runs through the two CuO_2 planes. The distance between the copper atom in the in these planes make it easier for charge to expectation between ions than from plane to plane. In between these conduction layers there are Barium, Yttrium and supplementary copper oxygen pairs. However these layers are not where current runs through the material, they play an important part in superconductivity [16].

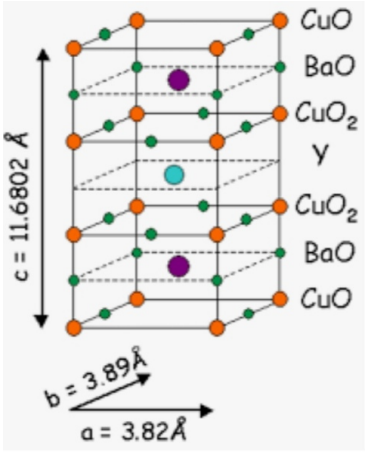

Fig. (2.1) Structure of YBCO

2.6 Defects on YBCO:

YBCO is a high temperature superconductor and till the discovered the high temperature superconductor structure is very complex and sophisticated feature comparing with all the other superconductors. There are many atoms bonded such a manner that changes the properties of the superconductors, especially in copper oxide superconductors [17]. After the discovery of cuprate superconductors explains that the defects plays significant role for governing the superconducting parameter of the system. In YBCO the defect is due to the oxygen deficiency in the crystal structure. The basal plane structure of the chain of CuO - CuO and between the Cu ions there are no any oxygen. Most of the materials defects can be increased by the doping but in the high temperature superconductor result is surprising that the defects are varying due the structure of CuO_2 conduction planes. The structural transition from orthorhombic to tetragonal is also happen due to the oxygen deficiency in the high temperature superconductors [17].

2.7 Vortex pinning effect:

There is a small gap between the normal and superconducting state is called the vortex state or mixed state. The normal, vortex and superconducting are basically in the type II superconductors. The normal core set in superconducting materials. In the normal state of microscopic is encircled by the conducting currents. In the normal states, the field penetrates of the of vortex lines in the mixed or vortex state. The every vortex lines has a core radius. The field is maximum at the center of materials and it is falls to 1/e times of the maximum field at the distance from the center. The flux vertex is known as fucoid. The fucoid brings quantum magnetic flux [15].

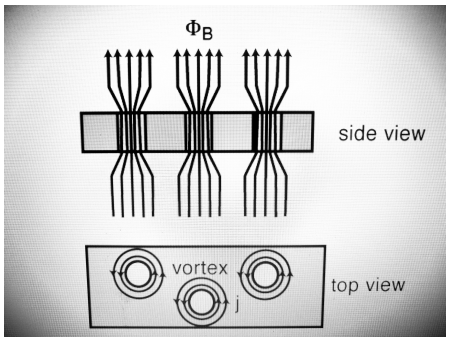

Fig(2.2) pinning effect

The idea of the vortex in ideal materials would be equal spacing. The crystal inhomogeneous in the real materials that's why the formation of vortex in the superconductivity. The question arises that at the mixed state the still take into account the perfect conductivity. The Lorentz force is acting on the vortex or pinning sites in mixed state due to the inhomogeneous of the real materials. The dissipation force is due the vortex motion governed to destruction of superconductivity. The understanding of the role of the fluctuation in the superconductor may be destroy the superconducting state. The fluctuation effect is a static property, which depend on the electrical and thermal conduction of the planes. According to the Ginzberg and Landau theory the electron density of the superconductor is proportional to the magnitude square of the complex wave function in the superconducting state. From this theory the flux $\varphi 0 = hc/2e$, 2e is due to the conduction of the Cooper pair. If the magnetic field is applied the superconducting rings are in normal state. When cooling the ring lower than the transition temperature, the flux is excluded from the ring but passes through the hole. If the external applied magnetic field off the flux through the hole remains

trapped. The super- current generated around the ring maintains the flux through the hole of the ring [18].

2.8 Aim of the Work:

1. Synthesis and study the structural, optical, and electrical properties of pure Yttrium Barium Copper Oxide (YBCO) and doping with Aluminum oxide AL_2O_3 at Room Temperature.
2. The manufacturing superconducting compounds for systems $YBa_2Cu_3O_7$ System.
3. To study their properties for pure YBCO (structural, optical, and electrical).

4. To Study effect add aluminum oxide (AL_2O_3) on structural, optical, and electrical properties.

CHAPTER THREE

3.0 Experimental Procedure

3.1 Introduction:

This chapter includes the preparation methods of the compositions pure $YBa_2Cu_3O_7$ and $YBa_2Cu_3O_7$ doped with AL_2O_3**.** So it contains important measurements to examine the properties of the samples, such as X-ray diffraction (XRD), FTIR, electrical, Scanning Electron Microscope (SEM), optical.

3.2 Sample Preparation

The samples YBCO were prepared by a solid state reaction by two methods [sintering samples in air, then mixing them with Aluminum Oxide],using appropriate weights of highly pure materials Y_2O_3, Ba_3CO, CuO, and AL_2O_3 powders. In proportion to their molecular weights, the total weight of the compounds was calculated as follow:

A- First step:

Measuring the weight of each reactant by using a sensitive balance with 4-digit type (KERN).

Powder name	Atomic Weight (gm)
Y_2O_3	0.4539
Ba_3Co	1.5867
CuO	0.9594
AL_2O_3	0.0900

B- Second step:

Synthesis of YBCO superconductor:

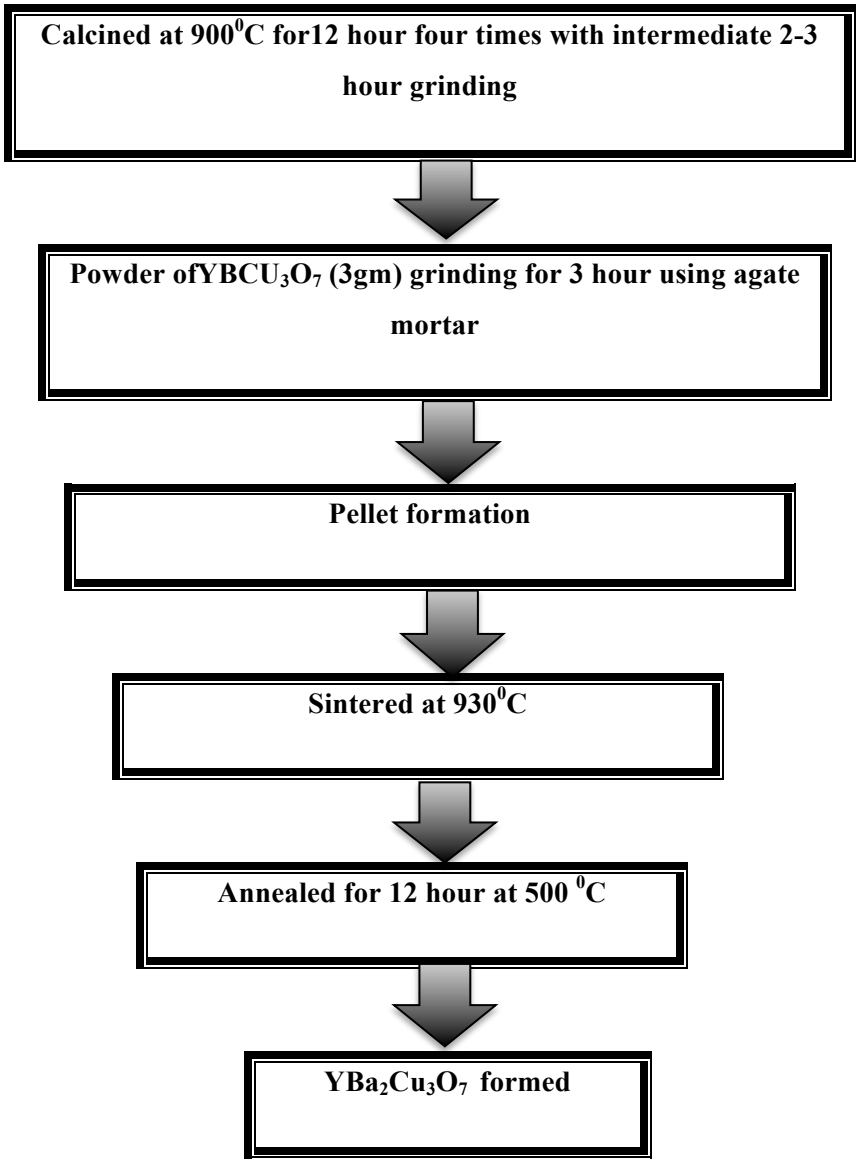

Stoichiometric amount of Yttrium Oxide, Barium Carbonate and Copper Oxide was taken as precursors to obtain the desire material YBCO.

$$Y_2O_3 + 2BaCO_3 + 3CuO \; 2YBa_2Cu_3O_7 \; \ldots\ldots\ldots(3.1)$$

The ingredients were grounded together in an agate mortar for 2-3 hrs to obtain a homogeneous mixture. After grinding, the powder was claimed at

900 0C in a muffle furnace for 12 hour and then the claimed powder was again heated for 4-5 times with intermediate grinding at the same temp.. After repeated heating, the resultant powder obtained, is pressed into pellets of 1mm thickness and finally sintered at 930 0C for 12 hrs and followed by oxygen annealing for 12 hrs for Oxygen uptake and thus obtained the resultant YBCO.

C- Three step:

Sample	$YBa_2Cu_3O_7$ (gm)	AL_2O_3 (gm)	The percentage of doped
S_1	0.500	0	%100
S_2	0.485	0.015	%3
S_3	0.470	0.030	%6
S_4	0.455	0.045	%9

Table (1) volumetric of powder used forsample preparation

3.3 Devices and measurements:

3.3.1 X-Ray Diffraction:

The structure of the appropriate weight of pure material and prepped samples were obtained by using X-ray diffractometer type (Shimadzu) having the following features was used to examine the structure of prepared samples. Source: CuKα , Voltage: 40kV, Current:. 0.30 mA , Wavelength: 1.5406A^0. X-ray diffraction patterns of pure materials

Y2O3,BaO . Positions and intensities of the diffraction peaks reveals that all our materials mainly consists of single phase.

Fig (3.1) Broker D8 focusing X-ray diffractometer

3.3.2 Scanning Electron Microscopy (SEM):

Scanning electron microscope (SEM) type (Bruker Nano GmbH, Germany) was used to study the nature of grains and analyze the surface morphology of the specimens of the composition YBCO with composite for sintering time 120h and sintering temperature 750°C.

Fig (3.2) Scanning Electron Microscope

3.3 .3 Electrical measurements

3.3.3.1 I-V measurement technique:

The experimental set up for performing I-V measurement was same as in the case of R-T measurement; but the purpose of measurement of this quiet different. Here we measure current against the voltage at fixed temperature to calculate a most valuable parameter Jc, which is the critical current density. The intercept of the I-V curve will give me critical current I_0 and the by using the formula current per unit area we can calculate current density (Jc) at different sample from the constant temperature (Room Temperature) in the superconducting state.

3.3.3. 2 Resistivity and Electrical conductivity Measurement:

The electrical resistance of a wire would be expected to be greater for a longer wire, less for a wire of larger cross sectional area, and would be expected to depend upon the material out of which the wire is made. Experimentally, the dependence upon these properties is a straightforward one for a wide range of conditions, and the resistance of a wire can be expressed as

$$R = \frac{\rho L}{A} \quad \text{……..(3.2)}$$

(ρ) Resistivity, (L) length, (A) cross sectional area. The factor in the resistance, which takes into account the nature of the material, is the resistivity. Although it is temperature dependent, it can be used at a given temperature to calculate the resistance of a wire of given geometry. It should be noted that it is being presumed that the current is uniform across the cross-section of the wire, which is true only for Direct Current. For

Alternating Current there is the phenomenon of "skin effect" in which the current density is maximum at the maximum radius of the wire and drops for smaller radii within the wire. At radio frequencies, this becomes a major factor in design because the outer part of a wire or cable carries most of the current. The inverse of resistivity is called conductivity(σ). There are contexts where the use of conductivity is more convenient.

$$\sigma = \frac{1}{\rho} \qquad \text{.....(3.3)}$$

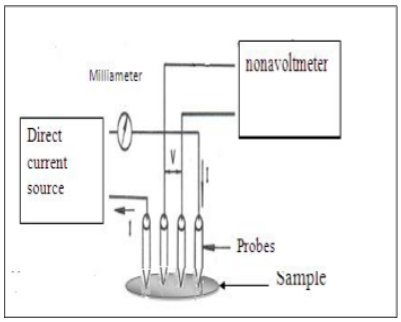

Fig (3.3) Circuit diagram of the sample of Resistivity Measurement

3.3.4 Ultraviolet-visible Spectrophotometry (UV/VIS):

UV-Visible spectrophtometer type UV-1800,complies with requirements of the EMC Directive 2004/108/EC and low Voltage Directive 2006/95/EC Manufacturer shimadzu corporation analytical and measuring instruments division. Ultraviolet-visible spectroscopy is considered an important tool in analytical chemistry. In fact, this is one of the most commonly used techniques in clinical as well as chemical laboratories. This tool is used for the qualitative analysis and identification of chemicals. However, its main use is for the quantitative determination of different organic and inorganic compounds in Solution. UV spectrophotometer principle follows the Beer-Lambert Law This law states that whenever a beam of monochromatic light is passed through a solution with an absorbing substance, the decreasing rate

of the radiation intensity along with the thickness of the absorbing solution is actually proportional to the concentration of the solution and the incident radiation.

Fig (3.4) UV-Visible spectrophtometer

3.3.5 optical measurements:

3.3.5.1 Optical Absorbance:

Absorbance (A), also known as optical density (OD), is the quantity of light absorbed by a solution. Transmittance is the quantity of light that passes through a solution. Absorbance and% transmittance are often used in spectrophotometry and can be expressed by the following

$$A = \text{Log } I_0 \ (\frac{I_\circ}{I}) \quad \ldots\ldots(3.4)$$

where I_0 is the intensity through the sample

$$T = I/I_0 \text{ and } \%T = 100\ (T) \quad \ldots\ldots\ldots(3.5)$$

The equation that allows one to calculate absorbance from % transmittance is

$$A = 2 - \log10\ (\%T) \quad \ldots\ldots\ldots\ldots (3.6)$$

Determine concentration using the Beer-Lambert Law The concentration of a sample can be calculated from its absorbance using the Beer–Lambert.

$$A = \varepsilon \times C \times P \quad \ldots\ldots\ldots\ldots (3.7)$$

Where ε is the molar absorptivity, or molar extinction coefficient, in L mol^{-1} cm^{-1} c is the concentration of the solute in solution, in mol/L p is the path length of the sample, in cm, for example 1 cm for a cuvette. of the incident light, and I is intensity of that light after it passed.

3.3.5.2 Optical Transmittance:

transmittance is defined as the ratio of transmitted optical power to the incident optical power for some object, for example an optical system. For transmission through flat unstructured surfaces, it is the same as the transmissivity. However, the transmittance is a more general term and can be specified in a wider range of situation. Some objects can cause scattering of light. One may then specify the hemispherical transmittance, which is based on the total transmitted radiant flux. Also, there is the directional transmittance, defined as the ratio of transmitted and incident radiance; it is a function of observation angle. There are extended objects, where light can penetrate, is internally scattered and thus partially transmitted and partially reflected. The transmittance simply quantifies the amount of light getting through the object, on whatever ways. When light is incident on a transparent plate with parallel surfaces, for example, Fresnel reflections occur on both surfaces. Interference effects, making the transmittance strongly wavelength-dependent, can affect the transmitted power. The results of transmission measurements with spectrophotometers, for example, are usually called transmittance rather than transmissivity, since one is often

dealing with extended samples. The formula for calculating transmittance (T) is transmittance equals light exiting the sample (I_T) divided by light striking the sample (I_0).

$$T = \frac{I_T}{I_\circ} \quad \text{.....(3.8)}$$

Transmittance usually is reported as percent transmittance, so the ratio is multiplied by 100, as:

$$\%T = \frac{I_T}{I_\circ} \times 100 \quad \text{.....(3.9)}$$

The Transmittance depends on the absorbance (A):

$$T = 10^{(2-A)} \quad \text{.....(3.10)}$$

3.3.5.3 Optical Reflectance:

reflectance is defined as the ratio of reflected radiant flux (optical power) to the incident flux at a reflecting object – for example, an optical component or system. It generally depends on the direction of incident light and on the optical frequency or wavelength. For polychromatic light, a total reflectance can be calculated with a given optical spectrum as a weighted average. The reflectivity(R) can be calculated according to the law of energy conservation and by knowing the value of each transmittance(T) and Absorbance (A).

$$R + A + T = 1 \quad \text{.....(3.11)}$$

3.3.5.4 Optical Energy Gap:

In solid-state physics, a band gap, also called an energy gap, is an energy range in a solid where no electronic states can exist. In graphs of the electronic band structure of solids, the band gap generally refers to the energy difference (in electron volts) between the top of the valence band and the bottom of the conduction band in insulators and semiconductors. It is the

energy required to promote a valence electron bound to an atom to become a conduction electron, which is free to move within the crystal lattice and serve as a charge carrier to conduct electric current.

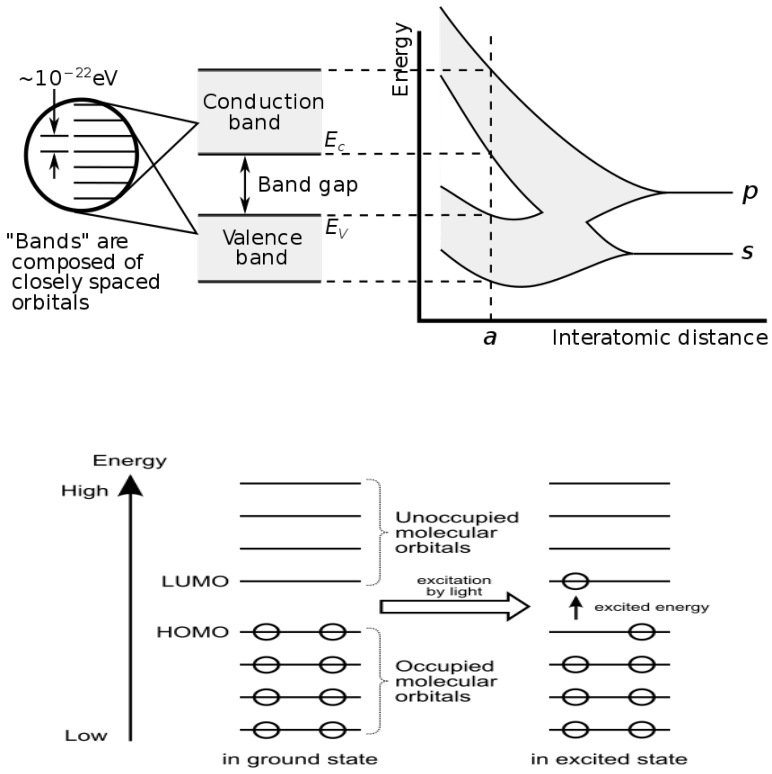

Fig (3.5) HOMO/LUMO gap in chemistry

It is closely related to the HOMO/LUMO gap in chemistry. If the valence band is completely full and the conduction band is completely empty, then electrons cannot move in the solid; however, if some electrons transfer from the valence to the conduction band, then current can flow (see carrier generation and recombination). Therefore, the band gap is a major factor determining the electrical conductivity of a solid. Substances with large band gaps are generally insulators, those with smaller band gaps are semiconductors, while conductors either have very small band gaps or none, because the valence and conduction bands overlap.

Experimentally, You can get the value of Eg by usually use the Tauc relation, which is given byBthis equation:

$$(\alpha h\nu)^n = c\,(h\nu - Eg)^n \quad \text{.....(3.12)}$$

where α is absorption coefficient given by

$$\alpha = 1/t \ln [(1-R)2 / T] \quad \text{.....(3.13)}$$

where t is the sample thickness, T and R are the transmission and reflection, while (hν) is the photon energy, where: hν(eV) = 1240 / [incident wavelength (nm)].

3.3.5.5 Optical conductfivity:

The optical response of a material is mainly studied in terms of the optical conductivity (σ)which is given by the relation

$$\sigma = \frac{\alpha\, n\, c}{\pi 4} \quad \text{.....(3.14)}$$

where c is the velocity of light,α is the absorption coefficient and n is the refractive index. It canbbe seen clearly that the optical conductivity directly depends on the absorption coefficient and the refractive index of the material.

3.3.6 Optical Constants:

3.3.6.1 Absorption Coefficient:

The absorption coefficient determines how far into a material light of a particular wavelength can penetrate before it is absorbed. In a material with a low absorption coefficient, light is only poorly absorbed, and if the material is thin enough, it will appear transparent to that wavelength. The absorption coefficient depends on the material and also on the wavelength of light which is being absorbed. Semiconductor materials have a sharp edge in their absorption coefficient, since light which has energy below the band gap does not have sufficient energy to excite an electron into the conduction band from the valence band. Consequently, this light is not absorbed. The absorption coefficient for several semiconductor materials is shown below. The probability of absorbing a photon depends on the likelihood of having a photon and an electron interact in such a way as to move from one energy band to another. For photons which have an energy very close to that of the band gap, the absorption is relatively low since only those electrons directly at the valence band edge can interact with the photon to cause absorption. As the photon energy increases, not just the electrons already having energy close to that of the band gap can interact with the photon. Therefore, a larger number of electrons can interact with the photon and result in the photon being absorbed. we know from Beer Lambert law

$$I=I_0 \exp(-\alpha \times t) \qquad \ldots\ldots.(3.15)$$

Thus,

$$\ln\left(\frac{I_o}{I}\right) = \alpha \times t \qquad \ldots\ldots\ldots (3.16)$$

$$\alpha = (2.303*A)/\ t \qquad \ldots\ldots\ (3.17)$$

where(I_0) incident intensity,(I) transmitted intensity (α) absorption coefficient,(t) Thickness of the material,(A) absorbance.

3.3.6.2 Refractive Index:

The refractive index determines how much the path of light is bent, or refracted, when entering a material. This is described by Snell's law of refraction.

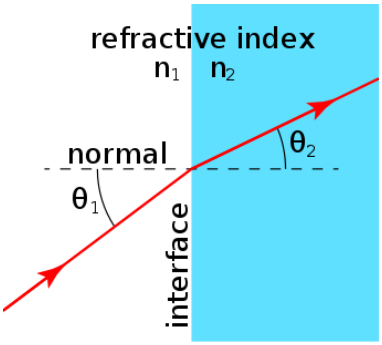

Fig (3.6) The refractive index described by Snell's law of refraction.

$$\mathbf{n_1 \sin\theta_1 = n_2 \sin\theta_2} \text{ ……..(3.18)}$$

Where θ_1 and θ_2 are the angles of incidence and refraction, respectively, of a ray crossing the interface between two media with refractive indices n_1 and n_2. The refractive indices also determine the amount of light that is reflected when reaching the interface, as well as the critical angle for total internal reflection, their intensity (Fresnel's equations) and Brewster's angle. The refractive index can be seen as the factor by which the speed and the wavelength of the radiation are reduced with respect to their vacuum values: the speed of light in a medium is

$$v = \frac{c}{n} \quad \text{……..(3.19)}$$

and similarly the wavelength in that medium is $\lambda = \frac{\lambda 0}{n}$, where λ_0 is the wavelength of that light in vacuum. This implies that vacuum has a refractive index of 1, and that the frequency

$$f = \frac{\nu}{\lambda} \quad \text{.....(3.20)}$$

of the wave is not affected by the refractive index. As a result, the perceived color of the refracted light to a human eye, which depends on the frequency, is not affected by the refraction or the refractive index of the medium. The refractive index depends on the type of material and the sphere structure, and is expressed in the following equation.

$$n = \left[\left(\frac{1+R}{1-R}\right)^2 - \left(K^2_{\circ} + 1\right)\right]½ + \frac{1+R}{1-R} \quad \text{.....(3.21)}$$

3.3.6.3 Extinction Coefficient:

As extinction coefficient (k) is a measure of light lost due to scattering and absorption per unit volume, hence, high values of k in lower wavelength range show that these films are opaque in this range. Oscillatory nature of the curve is a consequence of interference effect appears at higher wavelength range, which is known as extinction coefficient (k), is calculated from using the relation:

$$K = \frac{\alpha\lambda}{4\pi} \quad \text{..... (3.22)}$$

Where α is optical absorption coefficient.

3.3.7 Fourier Transform Infrared (FT-IR)

Fourier Transform-Infrared Spectroscopy (FTIR) is an analytical technique used to identify organic (and in some cases inorganic) materials. This

technique measures the absorption of infrared radiation by the sample material versus wavelength. The infrared absorption bands identify molecular components and structures. When a material is irradiated with infrared radiation, absorbed IR radiation usually excites molecules into a higher vibrational state. The wavelength of light absorbed by a particular molecule is a function of the energy difference between the at-rest and excited vibrational states. The wavelengths that are absorbed by the sample are characteristic of its molecular structure. The FTIR spectrometer uses an interferometer to modulate the wavelength from a broadband infrared source. A detector measures the intensity of transmitted or reflected light as a function of its wavelength. The signal obtained from the detector is an interferogram, which must be analyzed with a computer using Fourier transforms to obtain a single-beam infrared spectrum. The FTIR spectra are usually presented as plots of intensity versus wavenumber (in cm-1). Wavenumber is the reciprocal of the wavelength. The intensity can be plotted as the percentage of light transmittance or absorbance at each wavenumber.

Fig (3.7) Fourier Transform-Infrared Spectroscopy (FTIR)

CHAPTER FOER

4.0 Results and Discussion

4.1 Introduction:

This chapter describes synthesis and characterization of pure$YBa_2Cu_3O_7$ & $YBa_2Cu_3O_7$ doped with AL_2O_3. The first section investigates the influences of synthesis three phases of purity samples, including superconducting properties of $YBa_2Cu_3O_7$ systems (phase analysis, microstructures investigations, resistivity measurement, optical). The second section details the superconducting properties of $YBa_2Cu_3O_7$ doped with AL_2O_3 systems.

4.2 The properties of pure $YBa_2Cu_3O_7$ system:

4.2.1 crystal structures:

The X-ray diffraction (XRD) patterns for pure $YBa_2Cu_3O_7$ are shown in figure [(4.1)]. The positions and intensities of the diffraction peaks reveals that $YBa_2Cu_3O_7$ sample, minority CuBaO2 phase and a small amount of a minor unidentified

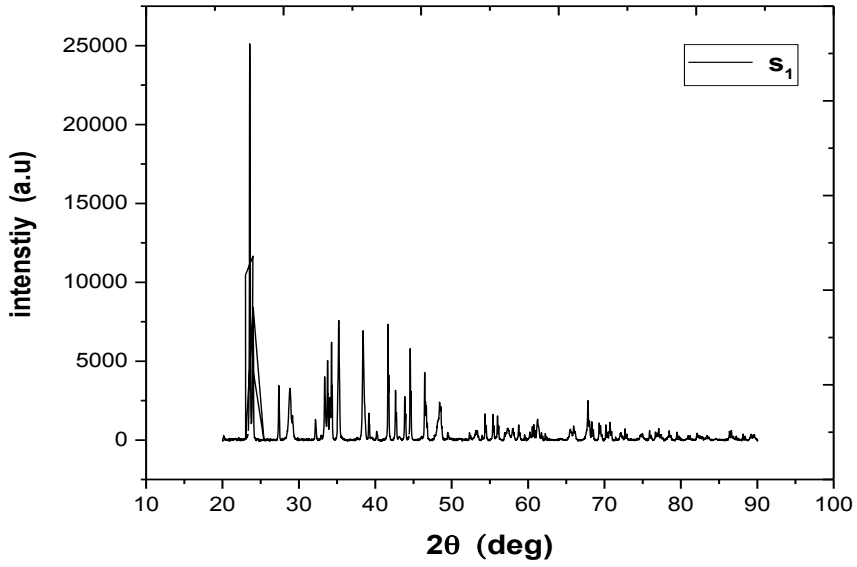

Fig (4.1) The X-ray diffraction (XRD) patterns for pure $YBa_2Cu_3O_7$

Peak N0	2Ɵ	β	D	h k l
1.	23.64227	0.67973	2.775562985	013
2.	23.84177	0.67982	3.553266877	001
3.	27.47948	0.67949	5.272122618	111
4.	28.87483	0.67951	6.899240083	120
5.	33.85089	0.67948	5.897495649	112
6.	34.29207	0.67949	15.41962281	110
7.	41.53557	0.67949	5.993096229	020
8.	42.83402	0.67941	2.43050637	200
9.	43.89535	0.67948	2.042519691	121

Lattice Constants:

Sample	a (A^0)	b (A^0)	c (A^0)	Volume (A^3)
S_1	3.5532	4.8610	11.9861	207.0251

$\alpha=\beta=\gamma=90^o$

Crystal Form: Orthorhombic – A-Center .

Space Group: (65) mm A.

Average Lattice Constants = 6 (A^0).

4.2.2 Scanning Electron Microscopy (SEM):

Micrographs of fractured surface for the samples with magnification (2mm,5μm,10 μm,500 μm) are shown in Figures.(4.2). The micrographs show of the one phases of (n=1,2,3,4) and their microstructures are characterized by elongated grains with no preferred orientation (randomly orientated).The shape of some grains are the plate-like is evident in (n=1). In n=3, layered structures have been alignment and grains become smaller with disappear the grain boundaries. Indeed grain boundaries inside the microstructure of the samples act as the barrier to scatter the conduction of carriers, the decrease of the number of grain boundaries lead to the reduction of this insulating region and thus enhanced the grain connectivity. The increase of the Ba-O layers yielded larger grains (larger crystallinities) as shown in Figs .(4.) for the samples at different (n).

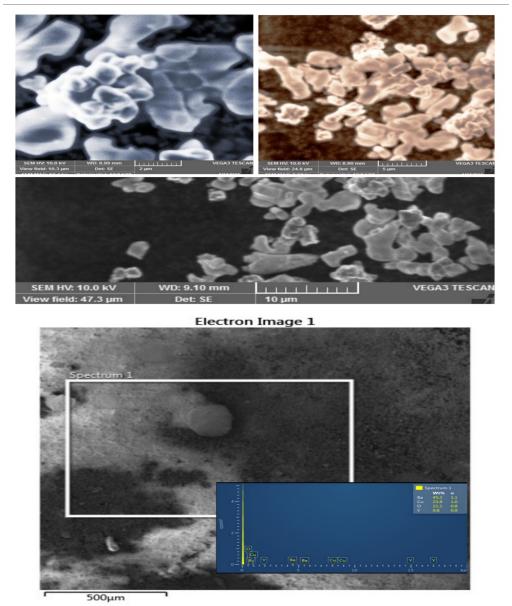

Figs. (4.2): SEM micrographs of the fracture surface of composites of pure YBCO

4.2.3Electrically properties.

4.2.3.1 I-V analysis:

In this measurement we applied current across two probes and voltage was measured at constant temperatures with the help of close cycle refrigerator. for pure $YBa_2Cu_3O_7$ The current was varying with the current source and calculated their corresponds voltage. From the figures at a certain temperature (30k) the critical current (Ic) is calculated. graph between current and voltage. From the table, we observed an increment of critical current density which is clearly shown in table below.

Ic=CriticaL Current(mA)	Jc=CURRENT DENSITY (A/m2)	ρ=Resistivity (Ωm)	σ= Conductivity
7	0.2147687×10^3	--	--
19	0.5829436×10^3	--	--
32	0.9817998×10^3	--	--
45	1.3806560×10^3	$0.10212536 \times 10^{-3}$	9.791887×10^3
50	1.5340623×10^3	0.0369851×10^{-3}	27.03915×10^3
70	2.1476872×10^3	0.0330284×10^{-3}	30.28624×10^3
80	2.4544997×10^3	0.0346736×10^{-3}	28.84038×10^3

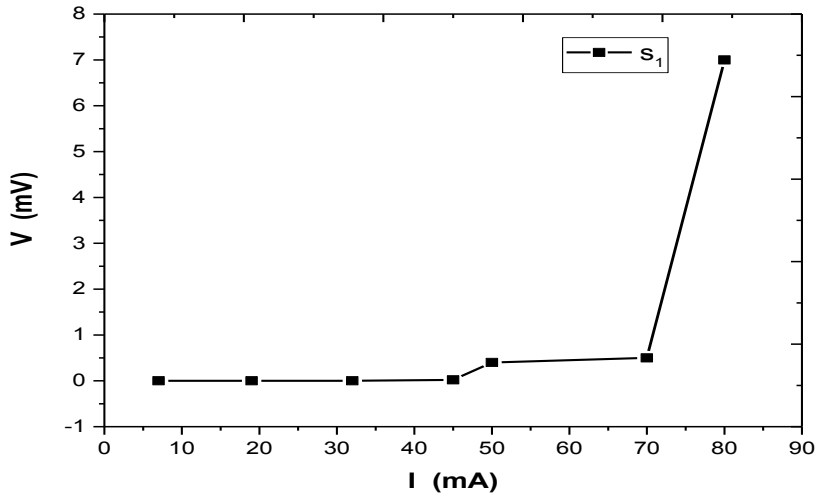

Fig (4.3) Graph between Current vs Voltage for Samples (s_1)at Room Tempertuer

4.2.4 optical properties:

4.2.4.1Optical Absorbance:

The Absorbance spectrum was measured as a function of wavelength of pure $YBa_2Cu_3O_7$ shown in figure [(4.1)] which represents Absorbance before doping it decreases and increases in range wavelength (200- 300)nm and then remains constant,as we can see from the figure below. The highest peak is intended for the highest absorption and the lowest for the lowest absorption. The table below shows the highest peak recorded and the lowest peak.

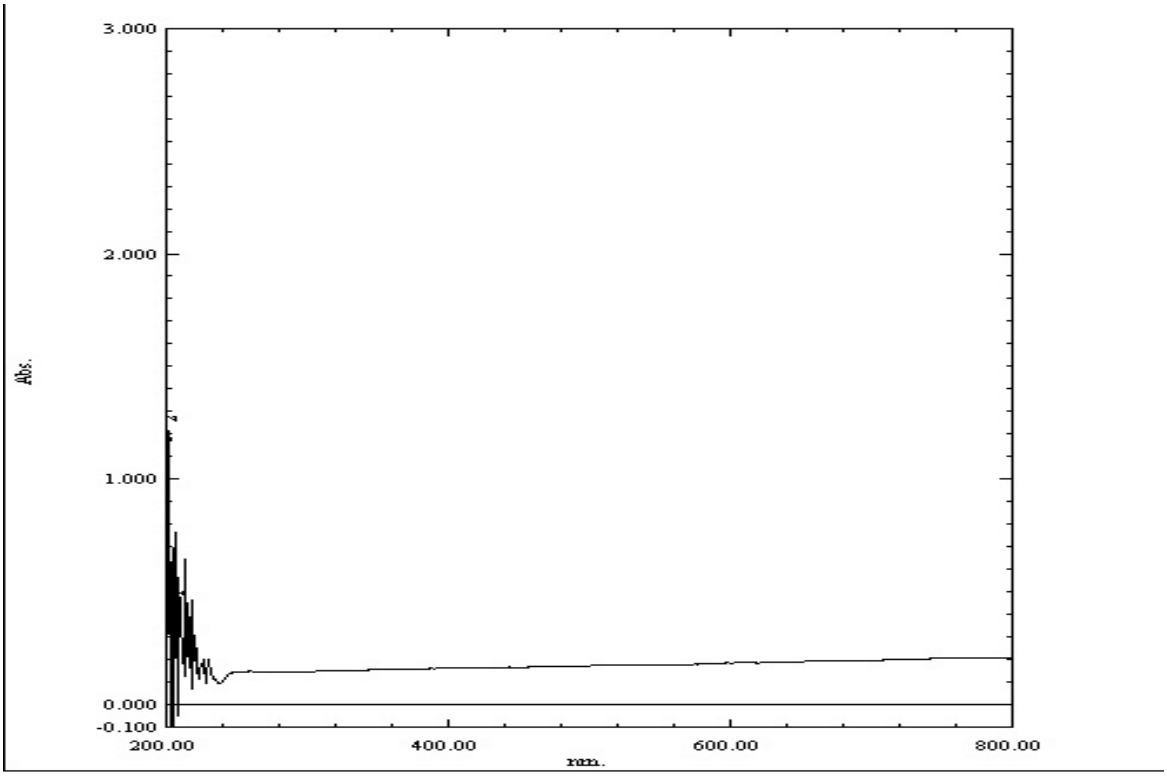

Fig (4.4) UV-vis –spectrometry spectrum of pure YBCO sample (s_1)

Table (2) UV-vis –spectrometry Spectrum description for pure YBCO sample (s_1)

N**o**	P**V**/	Wavelength (nm)	Abs. (a.u)	α (cm^{-1})	N	σ (s^{-1})
1	▲	206.00	0.372	0.8567	0.17882	36.5668×10^{8}
2	▲	202.00	1.144	2.634	0.5416	81.9615×10^{8}
3	▼	238.00	0.100	0.2303	0.1251	6.87690×10^{8}
4	▼	203.00	0.125	0.2878	0.1294	8.88928×10^{8}

4.2.4.2Optical Transmittance:

The Transmittance patterns of the pure $YBa_2Cu_3O_7$ samples is shown in figure [(4.1)], The figure shows the the transmittance as a function of the wavelength of pure $YBa_2Cu_3O_{7,}$ where we notice an increase and decrease in the transmittance with an increase in the wavelength in the range (200 – 300),and from there it gradually decreases.

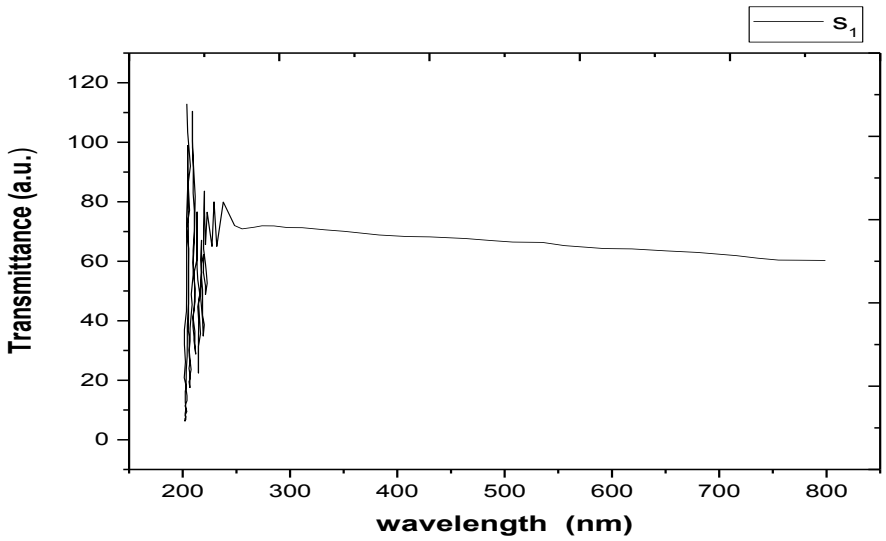

Fig (4.5) Transmittance spectrum of pure YBCO sample (s_1)

4.2.4.3Optical Reflectance:

The reflectance was calculated by using the transmittance and absorbance spectra based on the energy retention law, The figure shows the reflectance as a function of the wavelength of the pure $YBa_2Cu_3O_7$, where we obsrve an increase and decrease in the reflectance with an increase in the wavelength in the range (200 – 300),and from there it gradually increases.

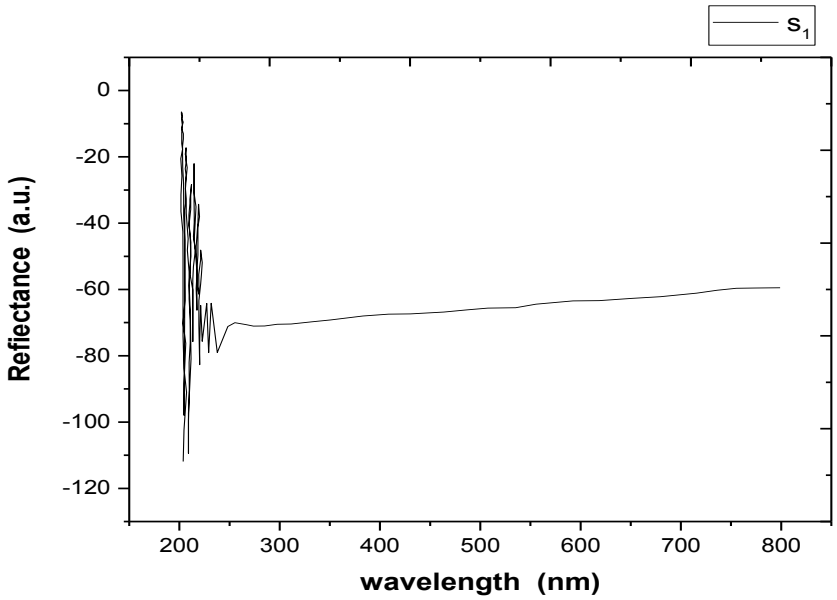

Fig (4.6) Reflectance spectrum of pure YBCO sample (s_1)

4.2.4.4Optical conductivity:

The optical conductivity was calculated for pure $YBa_2Cu_3O_7$, the figure below shows the change of the optical conductivity as function of wavelength for pure $YBa_2Cu_3O_7$, where we notice optical conductivity at highest value at λ=202.5 nm and then decrease with increase in the wavelength and at a specific point λ=214.79 nm the optical conductivity increase and then decrease and it remains constant with increase in the wavelength.

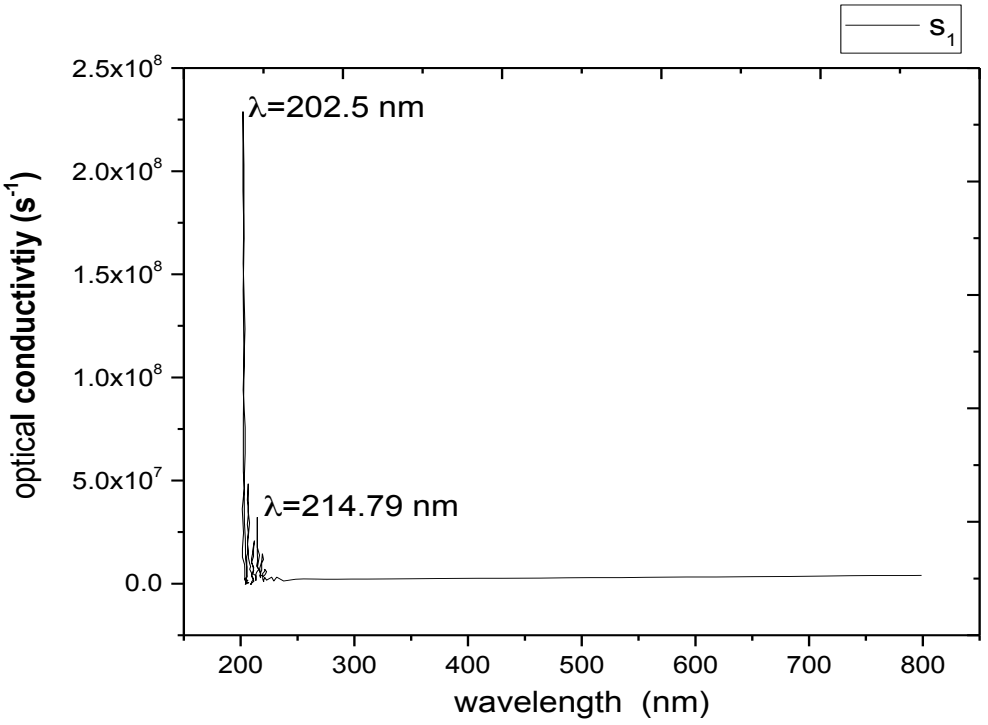

Fig (4.7)The optical conductivity spectrum of pure YBCO sample (s_1)

4.2.5Optical Constants:

4.2.5.1Absorption Coefficient:

The absorption Coefficient was calculated for pure $YBa_2Cu_3O_7$, the figure below shows the change of the absorption Coefficient as function of photon energy for pure $YBa_2Cu_3O_7$, where we notice decrease in absorption Coefficient with an increase in the wavelength and at a specific point a constant in the energy of photon and the absorption Coefficient until it reaches the highest energy, the absorption Coefficient begins to increase to its maximum degree.

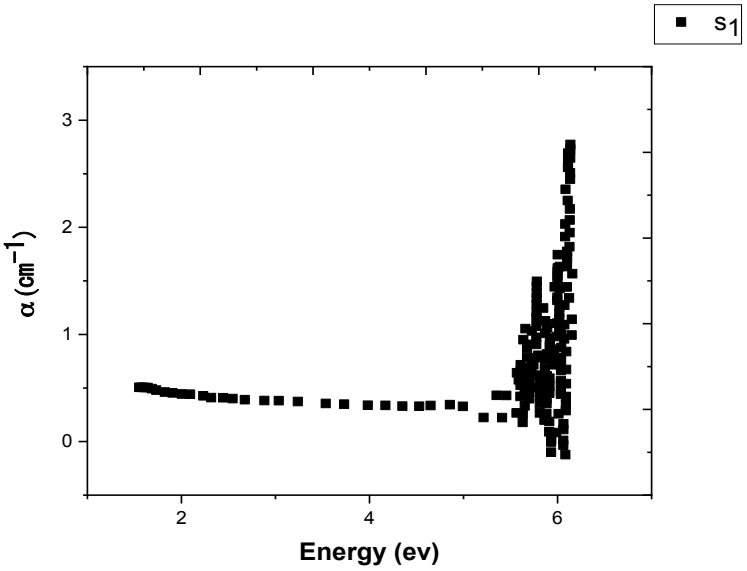

Fig (4.8) The absorption Coefficient spectrum of pure YBCO sample (s_1)

4.2.5.2 Refractive Index:

The refractive index was calculated for pure $YBa_2Cu_3O_7$, the figure below shows the change of the refractive index as function of photon energy for pure $YBa_2Cu_3O_7$, where we notice a constant in the energy of photon and the refractive index until it reaches the highest energy, the refractive index begins to increase to its maximum degree.

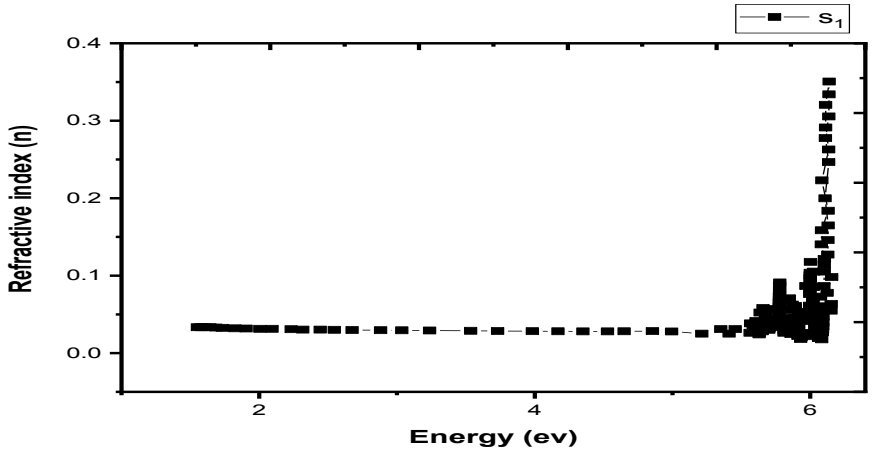

Fig (4.9) The refractive index spectrum of pure YBCO sample (s_1)

4.2.5.3Extinction Coefficient:

The extinction coefficient was calculated for pure $YBa_2Cu_3O_7$, the figure below shows the change of the extinction coefficient s function of photon energy for pure $YBa_2Cu_3O_7$, where we notice extinction coefficient at highest value and then decrease gradually with increase in the wavelength and at a specific point a constant in the energy of photon and the absorption Coefficient until it reaches the highest energy, the absorption Coefficient begins to increase to its maximum degree.

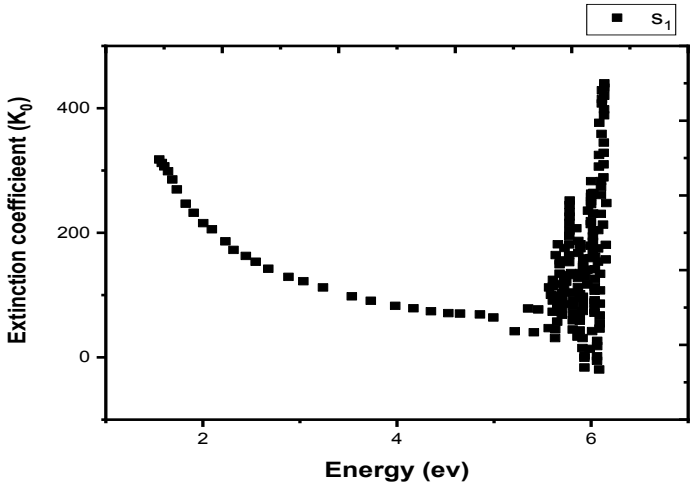

Fig (4.10) The extinction coefficient spectrum of pure YBCO sample (s_1)

4.3 Effect AL_2O_3 doped on The properties of YBCO systems

4.3.1 Scanning Electron Microscopy (SEM):

The figures ((4.11),(4.12)) shows the results of a Scanning Electron Microscopy (SEM) for YBa2Cu3O7 doped with AL_2O_3, where the images are shown as homogeneity increases and the crystal growth is practically evident.

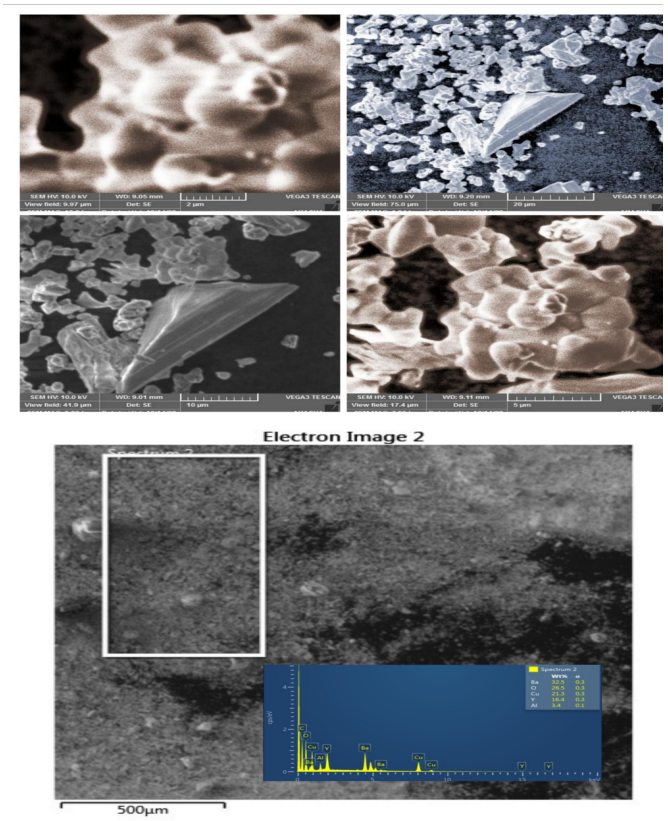

figure (4.11) The SEM image of $YBa_2Cu_3O_7$ doped with AL_2O_3e sample(s_2)

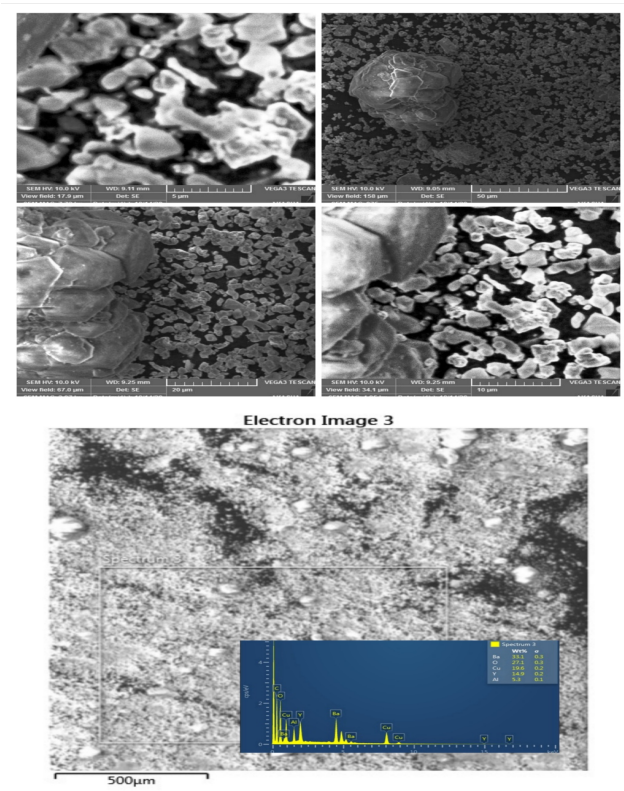

Figure (4.12) The SEM image of $YBa_2Cu_3O_7$ doped with AL_2O_3e sample (s_3)

4.3.3Electrically properties

4.3.3.1 I-V analysis:

In this measurement we applied current across two probes and voltage was measured at constant temperatures with the help of close cycle refrigerator for YBa2Cu3O7 doped with AL_2O_3. The current was varying with the current source and calculated their corresponds voltage. From the figures at a certain temperature the critical current (Ic) is calculated, Resistivity and electrical conductivity.

Ic= CriticaL Current(mA)	Jc=CURRENT DENSITY (A/m2)	ρ=Resistivity (Ωm)	σ= Conductivity
10	0.30681×10^3	--	--
20	0.61362×10^3	--	--
40	1.22724×10^3	--	--
50	1.53406×10^3	0.027738×10^3	36.051625×10^3
55	1.68746×10^3	0.033622×10^3	29.742430×10^3
60	1.84087×10^3	0.046231×10^3	21.630507×10^3
70	2.14768×10^3	0.056086×10^3	17.829761×10^3
75	2.30109×10^3	0.049174×10^3	20.335949×10^3
90	2.76131×10^3	0.041094×10^3	24.334452×10^3

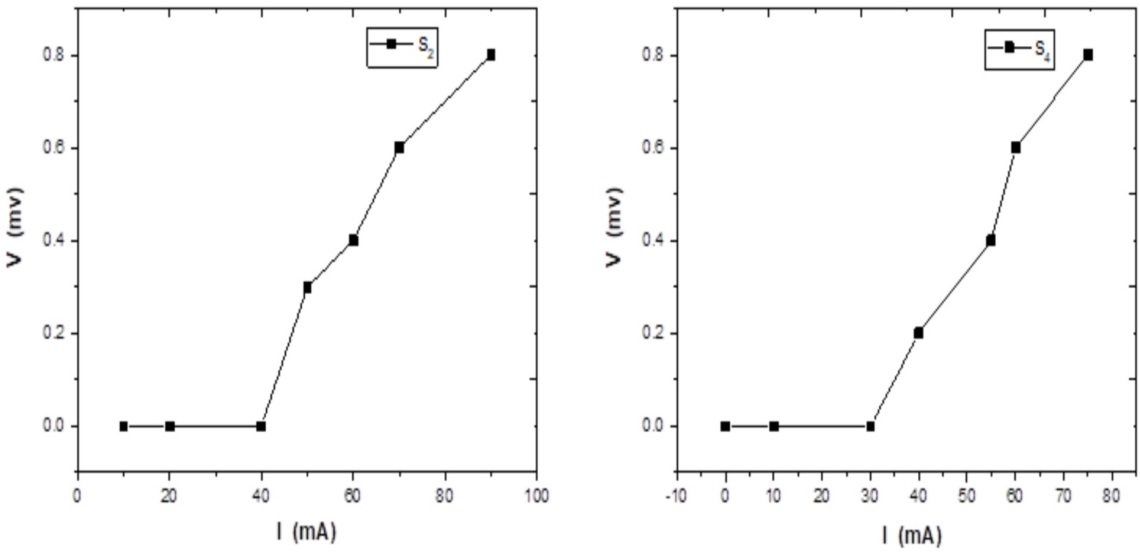

Fig (11) Graph between Current vs Voltage for samples (s_2,s_4)at room tempertuer

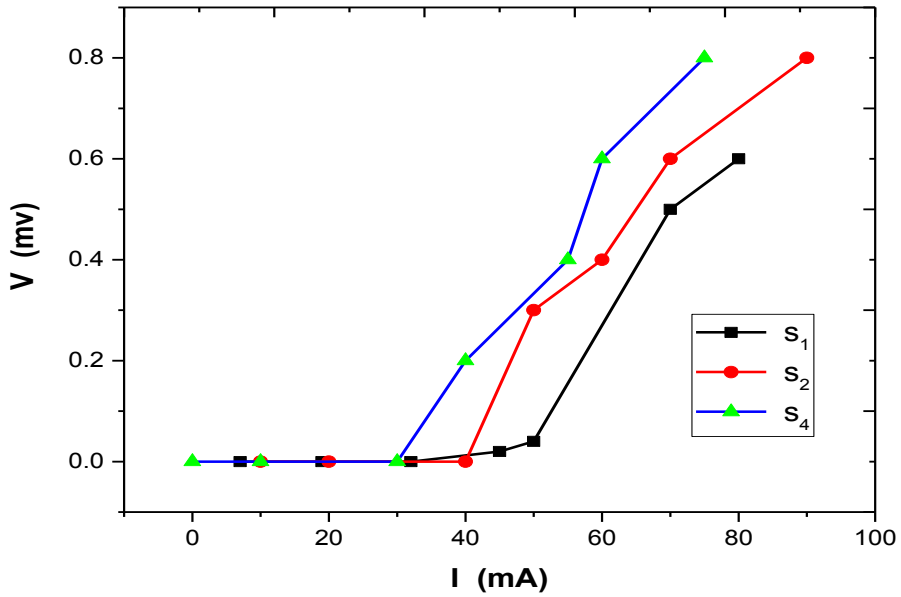

Fig (4.13) Comparision of graph between Current vs Voltage for all samples at room temperture

4.3.4 optical properties:

4.3.4.1Optical Absorbance:

The Absorbance spectrum was measured as a function of wavelength of $YBa_2Cu_3O_7$ doped with AL_2O_3 by volume ratio (0.015,0.03,0.045) shown in figure [(4.14)] which represents Absorbance after doping it decreases and increases in range wavelength (200- 300) nm and then remains constant, as we can see from the figure below. It turns otut that the absorption increases with increasing doped. from the figure we able to calculated absorption coefficient, refractive index and optical conductivity, we observed increment of an optical conductivity increases in absorbance.

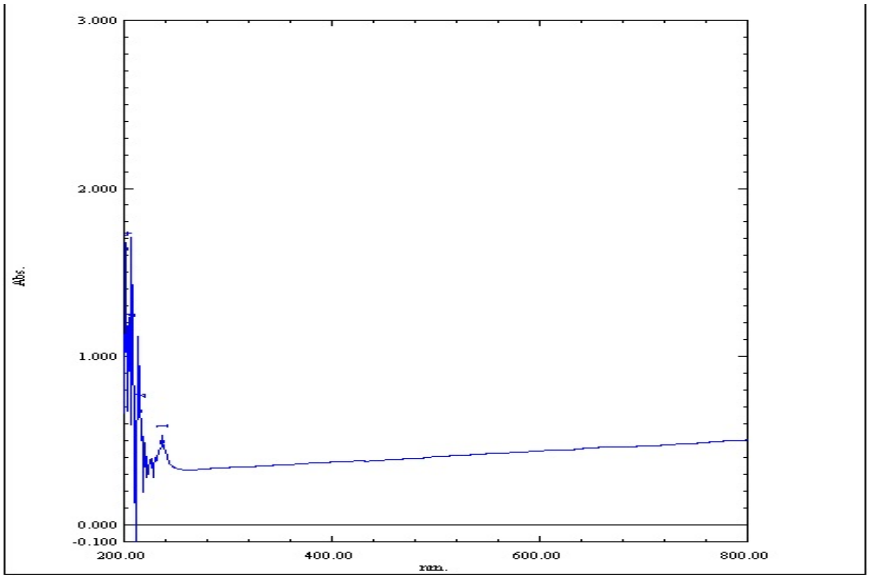

Fig (4.14) UV-vis –spectrometry spectrum of YBCO which dopped with AL_2O_3sample (s_2)

Table (3) UV-vis –spectrometry Spectrum description for YBCO which dopped with AL_2O_3sample (s_2):

No	Pv/	Wavelength (nm)	Abs.(a.u.)	α (cm^{-1})	N	σ (s^{-1})
1	↑	237	0.463	1.066	0.199	5.0500×10^{8}
2	↑	215	0.643	1.480	0.255	8.9842×10^{8}
3	↑	205	1.129	2.600	0.527	32.618×10^{8}
4	↑	201	1.611	3.710	1.238	109.33×10^{8}
5	↓	261	0.328	0.755	0.169	3.0374×10^{8}
6	↓	222	0.338	0.778	0.170	3.1485×10^{8}
7	↓	212	0.522	1.202	0.217	6.2093×10^{8}
8	↓	203	0.675	1.554	0.268	9.9144×10^{8}

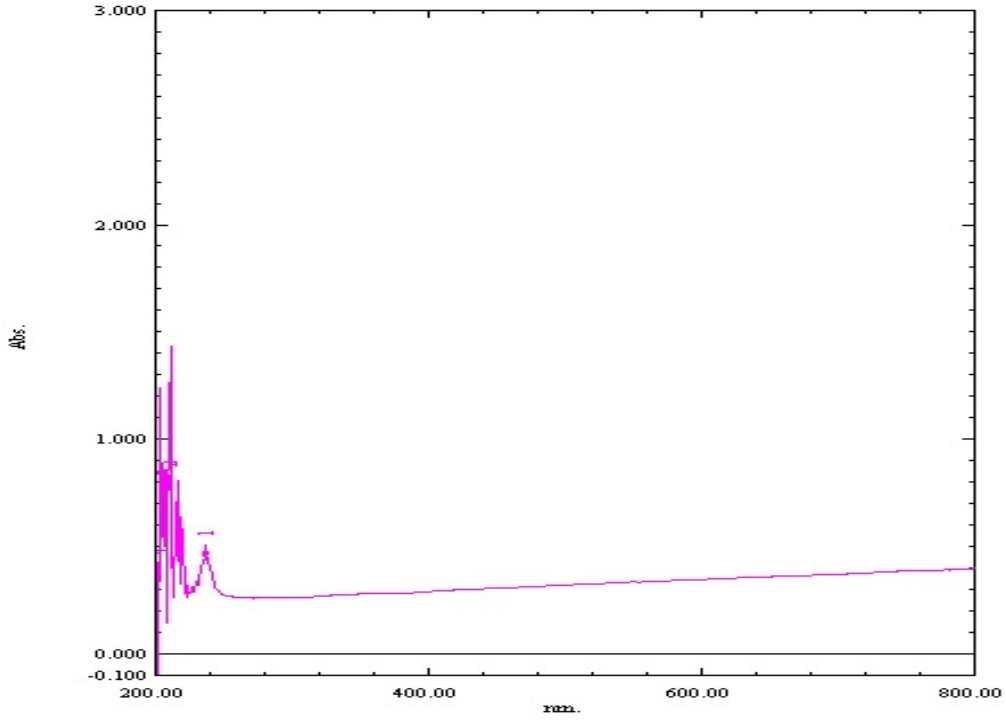

Fig (4.15) UV-vis –spectrometry spectrum of YBCO which dopped with AL_2O_3sample (s_3)

Table (4) UV-vis –spectrometry Spectrum description for YBCO which dopped with AL_2O_3sample(s_3):

No	Pv/	Wavelength (nm)	Abs.(a.u.)	α (cm^{-1})	N	σ (s^{-1})
1	↑	237	0.437	1.006	0.194	4.646×10^{8}
2	↑	210	0.764	1.759	0.304	12.729×10^{8}
3	↑	207	0.728	1.676	0.289	11.530×10^{8}
4	↑	201	0.357	0.822	0.173	3.3853×10^{8}
5	↓	225	0.294	0.677	0.160	2.5786×10^{8}
6	↓	202	0.324	0.746	0.165	2.9302×10^{8}

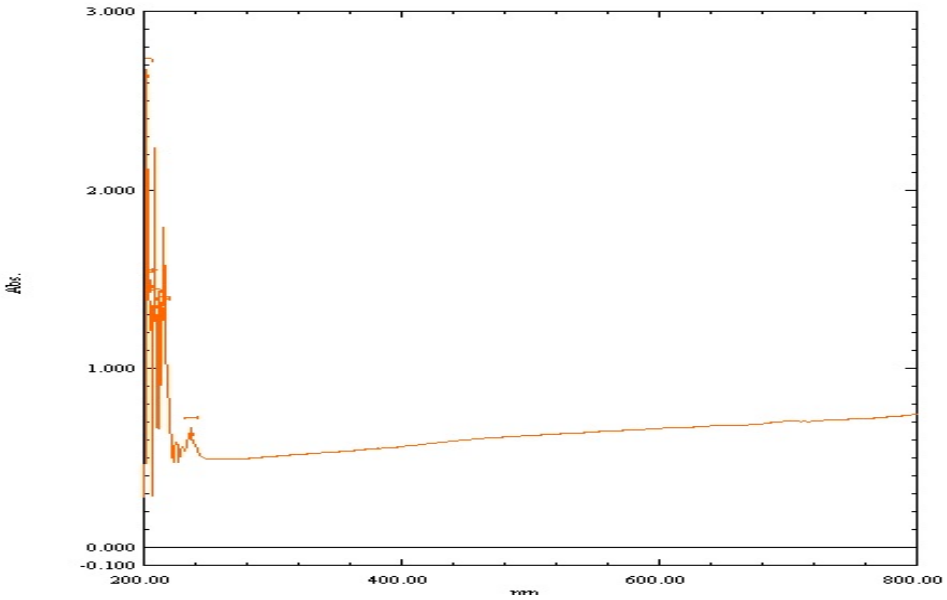

Fig (4.16) UV-vis –spectrometry spectrum of YBCO which dopped with AL_2O_3sample (s_4)

Table (5) UV-vis –spectrometry Spectrum description for YBCO which dopped with AL_2O_3sample (s_4):

No	Pv/	Wavelength (nm)	Abs.(a.u.)	α (cm^{-1})	n	σ (s^{-1})
1	↑	236	0.601	1.384	0.241	7.940×10^{8}
2	↑	215	1.274	2.934	0.667	46.587×10^{8}
3	↑	208	1.314	3.026	0.714	51.433×10^{8}
4	↑	205	1.426	3.284	0.868	67.858×10^{8}
5	↑	202	2.608	6.006	6.069	867.72×10^{8}
6	↓	255	0.492	1.133	0.542	14.618×10^{8}
7	↓	227	0.538	1.239	1.157	34.126×10^{8}
8	↓	211	1.196	2.754	0.588	38.549×10^{8}
9	↓	207	1.276	2.938	0.669	46.790×10^{8}
10	↓	204	1.415	3.258	0.744	57.703×10^{8}

4.3.4.2Optical Transmittance:

The Transmittance patterns of the $YBa_2Cu_3O_7$ doped with AL_2O_3samples is shown in figure [(4.1)], The figure shows the transmittance as a function of the wavelength of YBa2Cu3O7 doped with AL2O3,where we notice an increase and decrease in the transmittance with an increase in the wavelength in the range (200 – 300),and from there it gradually decreases. We also note that the transmittance in the third sample (s_3) is higher than in the second and fourth and the highest value shown in the second sample (s_2).

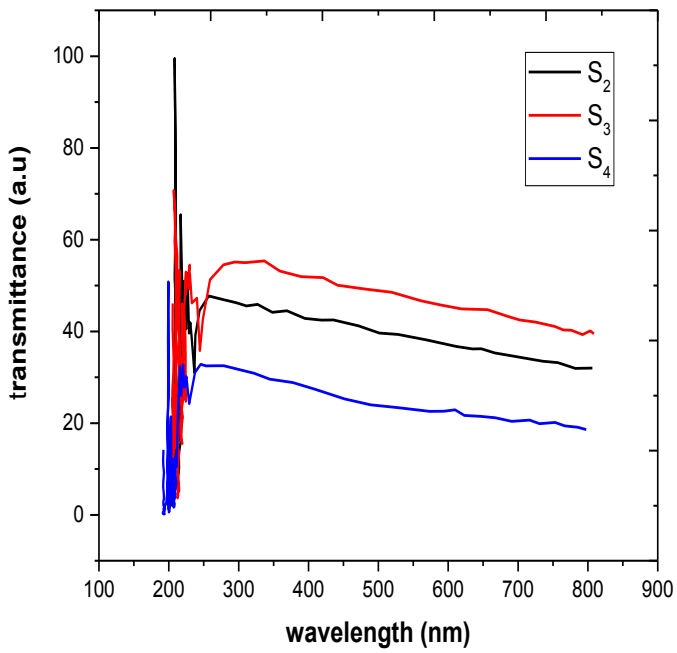

Fig (4.17) Transmittance spectrum of YBCO which dopped with AL_2O_3

4.3.4.3 Optical Reflectance:

The reflectance was calculated by using the transmittance and absorbance spectra based on the energy retention law, The figure shows the reflectance as a function of the wavelength of the $YBa_2Cu_3O_7$ doped with AL_2O_3samples is shown in figure [(4.18)], where we observe an increase and decrease in the reflectance with an increase in the wavelength in the range (200 – 300),and from there it gradually increases, from there it gradually decreases. We also note that the transmittance in the third sample (s_3) is higher than in the second and fourth and the highest value shown in the second sample (s_2).

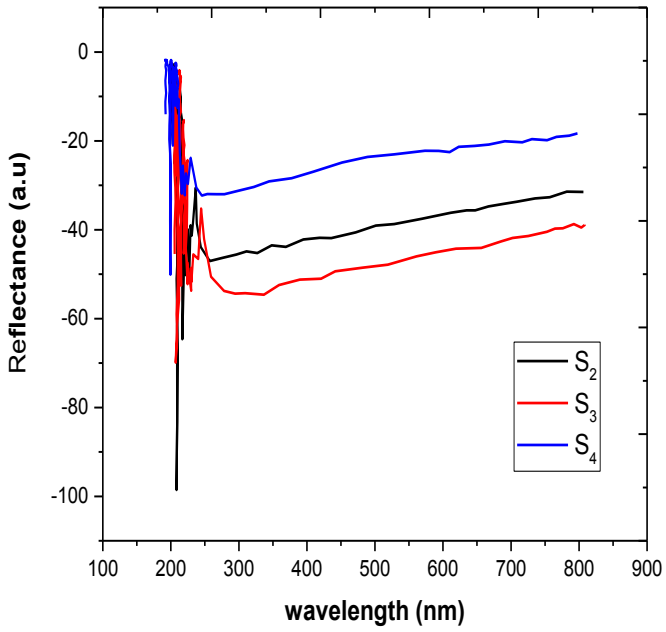

Fig (4.18) Reflectance spectrum of YBCO which dopped with AL_2O_3

4.3.4.4 Optical Constants:

1) Absorption Coefficient:

The absorption Coefficient was calculated for $YBa_2Cu_3O_7$ doped with AL_2O_3samples is shown in figure [(4.19)], the figure below shows the change of the absorption Coefficient as function of photon energy for pure $YBa_2Cu_3O_7$, where we notice decrease in absorption Coefficient with an increase in the wavelength and at a specific point a constant in the energy of photon and the absorption Coefficient until it reaches the highest energy, the absorption Coefficient begins to increase to its maximum degree. We also note that the absorption Coefficient in the third sample (s_3) is higher than in the second and fourth and the highest value shown in the second sample (s_2).

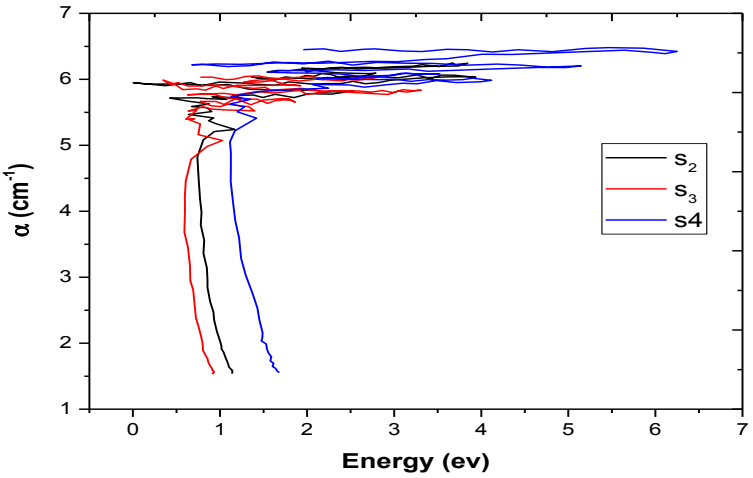

Fig (2.19) The absorption Coefficient spectrum of YBCO which dopped with AL_2O_3

2) Refractive Index:

The refractive index was calculated for $YBa_2Cu_3O_7$ doped with AL_2O_3samples is shown in figure [(4.20)], the figure below shows the change of the refractive index as function of photon energy for pure $YBa_2Cu_3O_7$ doped with AL_2O_3, where we notice a constant in maximum degree of refractive index and increase in the energy of photon until it reaches the highest energy in (s_3&s_4), and in (s_4) the refractive index is reduced to its lowest value with increase in energy of photon to maximum degree.

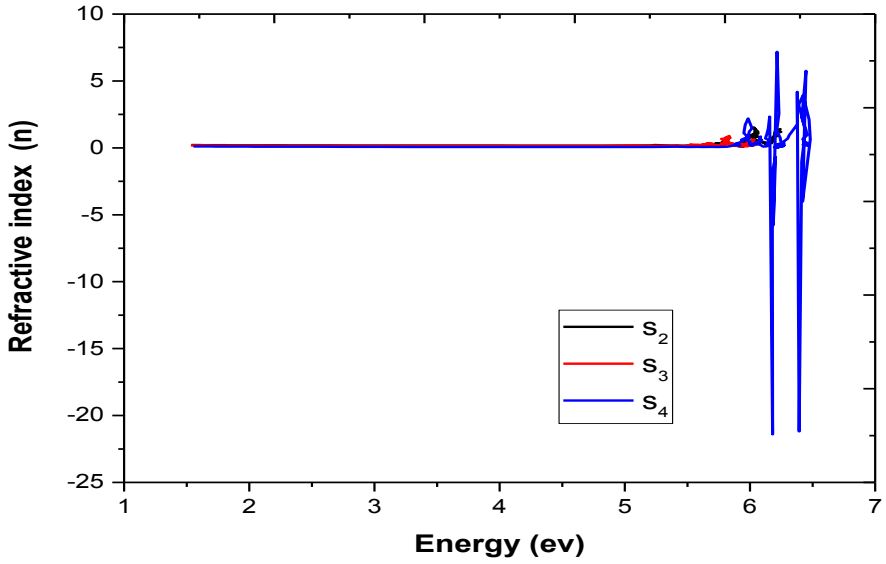

Fig (4.20) The refractive index spectrum of YBCO which dopped with AL_2O_3

3) Extinction Coefficient:

The extinction coefficient was calculated for $YBa_2Cu_3O_7$ doped with AL_2O_3 samples is shown in figure [(4.21)], the figure below shows the change of the extinction coefficient as function of photon energy for $YBa_2Cu_3O_7$ doped with AL_2O_3,where we notice extinction coefficient at highest value and then decrease gradually with increase in the energy of photon and at a specific point a constant in the energy of photon and the absorption Coefficient until it reaches the highest energy, the absorption Coefficient begins to increase to its maximum degree in (s_2&s_3)and at (s_4) it remains constant, this indicates that the greater the doped the less in extinction coefficient.

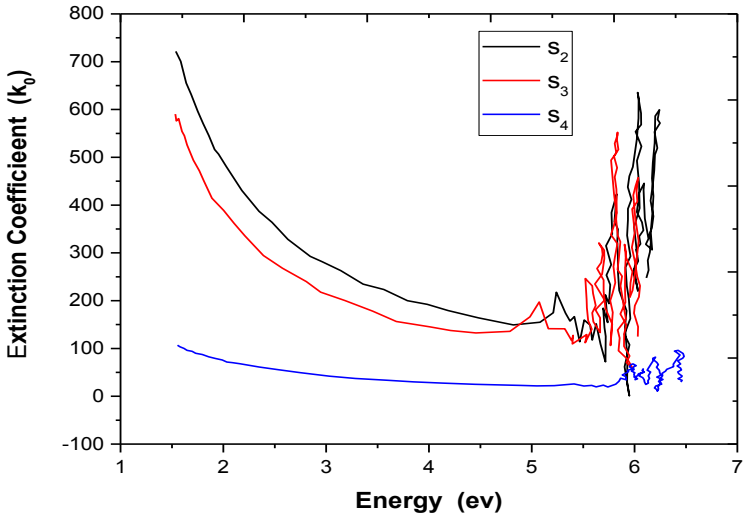

Fig (4.21) The extinction coefficient spectrum of YBCO which dopped with AL_2O_3

4.3.4.5 Optical Energy Gap:

The optical energy gap value was calculated for $YBa_2Cu_3O_7$ doped with AL_2O_3 samples is shown in figure [(4.22)], this is done through a graph between the energy value of the incident photon (hv) and $(\alpha hv)^2$ and by drawing the outer tangent of high absorption region of the curve to cross the energy axis of the photon at (y=0) where the point of intersection at x-axis is the value of the optical energy gap, through the figures (4.22), and the results are shown in the table (6) The optical energy gap less up doped, this is because the doped formed objective levels within the energy gap that led to the absorption of low-energy photons, thus reducing the energy gap.

Table (6) Energy gap values for the allowable electronic transition of pure YBCO and YBCO which dopped with AL_2O_3:

Sample	(Eg) pure eV	(Eg) doped eV
S_1	5.02	--
S_2	--	4.88
S_3	--	4.02
S_4	--	3.91

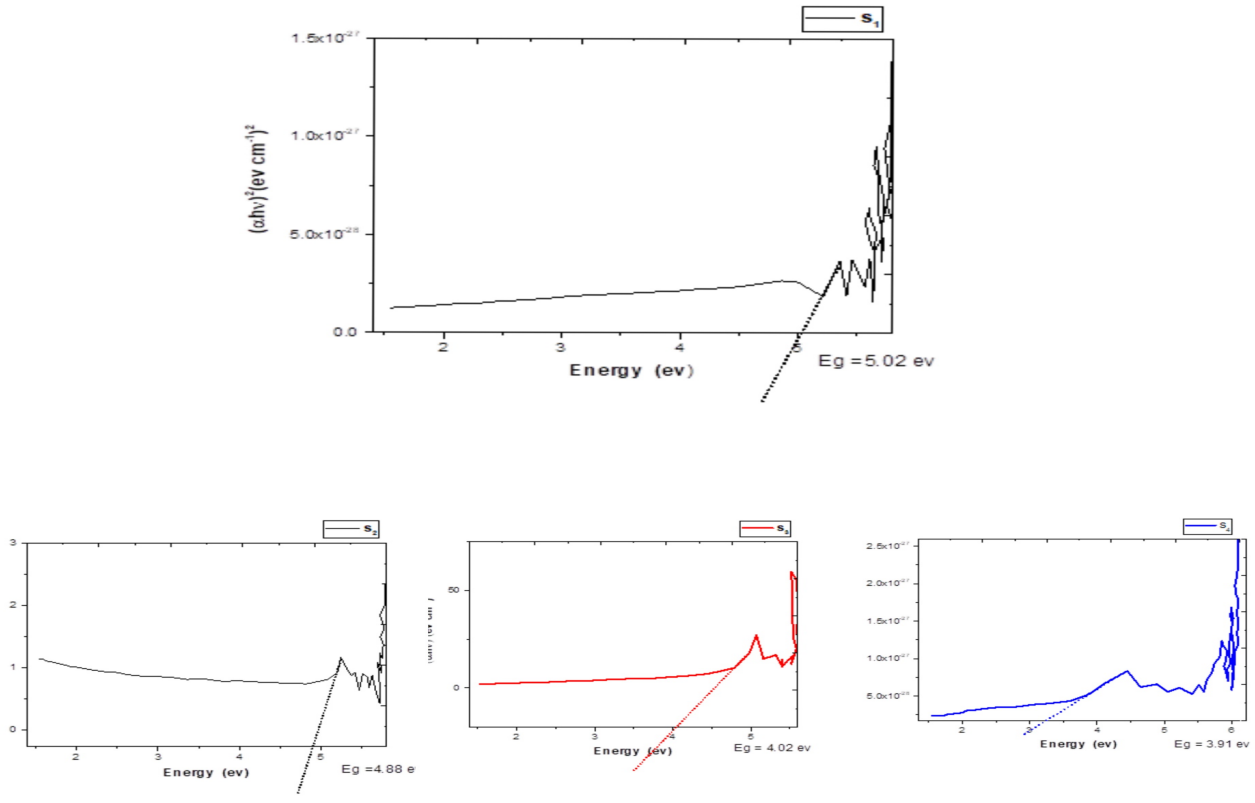

Fig (4.22) Energy gap values for the allowable electronic transition of pure YBCO and YBCO which dopped with AL_2O_3

4.3.4.6 Optical conductivity:

The optical conductivity was calculated for $YBa_2Cu_3O_7$ doped with AL_2O_3 samples is shown in figure [(4.23)], the figure below shows the change of the optical conductivity as function of wavelength for $YBa_2Cu_3O_7$ doped with AL_2O_3, where we notice optical conductivity at highest value in (s_2, s3,s4) continue to then increase with increase in the wavelength, and optical conductivity increase with doping at λ=202 nm optical conductivity highest value.

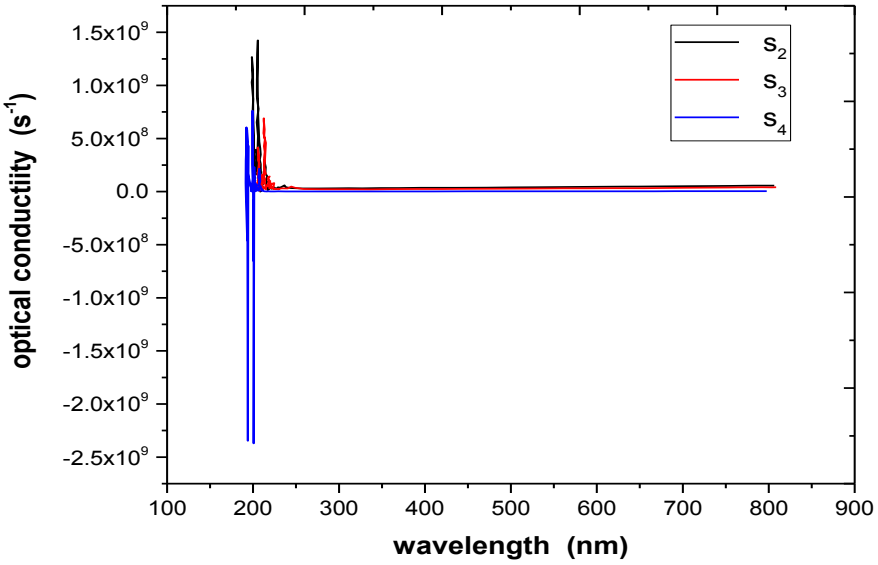

Fig (4.23) The optical conductivity spectrum of YBCO which dopped with AL_2O_3

4.3.5 Fourier Transform Infrared (FT-IR):

The IR spectroscopy has been studied for pure $YBa_2Cu_3O_7$ and doped with AL_2O_3 Infrared spectrum can be affected by several factors in the whole region from 500-4000 cm-1 such as the influence of different ambient conditions (humidity, temperature and pressure in the sample preparation), storing and processing that take place on the samples .The amount of moisture in the Potassium bromide matrix varied in the individual

laboratories. The Sample prepared at room temperature is shown in Figures ((4.24) , (4,25)). Where the percentage of transmittance is plotted as a function of wave number (cm^{-1}) The characteristic of FTIR can distinguish between sulfoxide and carbon dioxide in the (1000 - 2500) cm^{-1} region of the spectrum. This region of the spectrum is very important to distinguish and diagnostics the superconductor in both cases of doped and undoped.

Table (7): The list of the observed peaks for the prepared pure $YBa_2Cu_3O_7$ and doped with AL_2O_3 at Room Temperature:

The band's range (Cm-)	Assignment	Pure	Doped
422.52 – 500	(C-I) halo compound, stretching, strong	418.52 449.38 474.46	418.52 422.38
500 -750	(C-Br) halo compound, stretching, strong	557.39 634.45 667.32 692.40	530.39 692.40
750 – 1000	(C-C) bending, alkene, strong,vinylidene	856.34	856.34
1000 -1250	(S-O) stretching, strong,sulfoxide	1058.85	1058.85
1250 – 1500	(O-H) bending, medium,phenol	1390	1390
1500 – 1750	(C=C) stretching,strong,α,β-	1556.45	---

	unsaturated ketone		
≈ 1750	(C=O) stretching, strong,δ-lactone,esters	1749.32	1749.32
2000 – 25000	(O=C=O) stretching, strong,carbon dioxide	2356.85 2451.36	2451.36

Table (7) show the main transmission bands of the pure $YBa_2Cu_3O_7$ and doped with AL_2O_3. The observed peak at (418.52) cm^{-1} is a measure of the amount of iodo, which was returned to the used monomer (aniline hydrochloride). While the peak at (856.34)cm^{-1} could be related to the alkene in the case of undoped (pure), but it possible to return to each of the alkene and to vinylidene compounds which resulting from the dopant acidic. The most important characteristic bands of $YBa_2Cu_3O_7$ is the band observed at a wavelength of 1058.85 cm^{-1} and the band at 2451.36cm^{-1}, which represents the sulfoxide and carbon dioxide, respectively. Finally the other bands which located they presence the vibration bands of water molecules in most of the spectra shown in figure (4.24) correspond to a higher humidity during measurements that were made. When we comparing a doped with AL_2O_3 in fig (4.24) with the pure peaks Fig (4.25) we notice the change in intensity, no shifting in the position of the band, and the peak for sulfate group were noticed which mean the doping happened in $YBa_2Cu_3O_7$ chain.

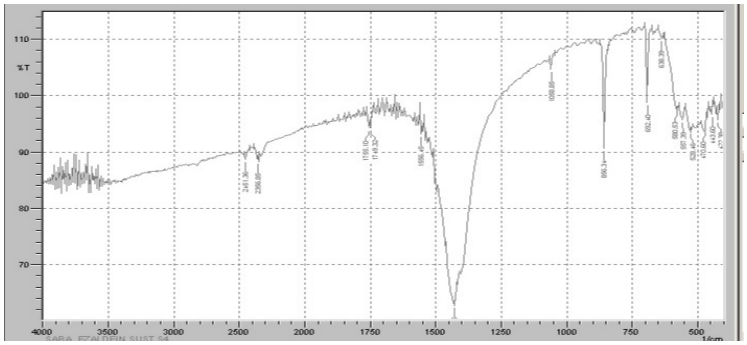

Fig (4.24): FTIR spectrum of the Pure YBCO

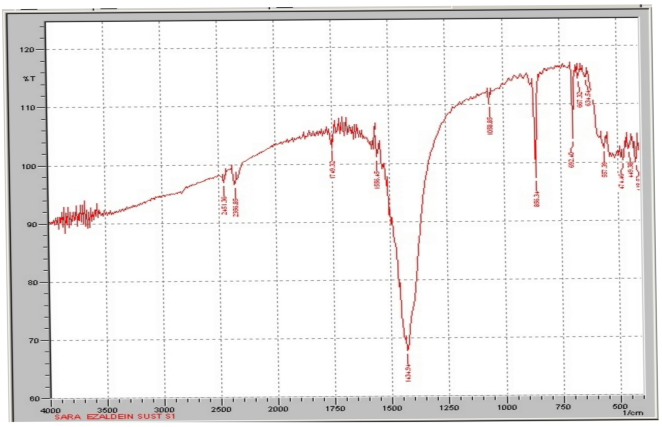

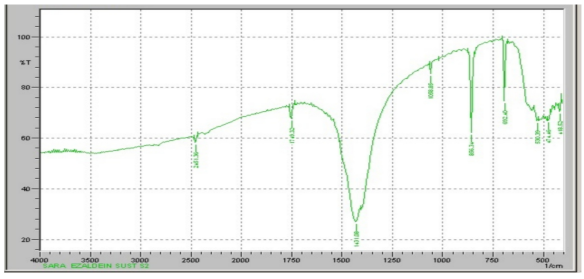

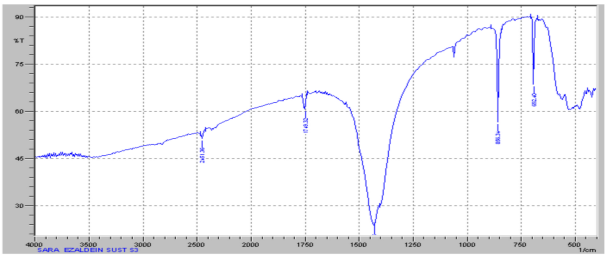

Fig (4.25): FTIR spectrum of the YBCO which dopped with AL_2O_3

4.4 Conclusion:

The YBCO superconductor is prepared successfully via solid state reaction method. XRD analyses of the crystal structure for pure $YBa_2Cu_3O_7$, is found to confirm the phase formation. The Fourier Transform Infrared spectrum showed that the $YBa_2Cu_3O_7$ is pure, and $YBa_2Cu_3O_7$ which doped with AL_2O_3 revealed perfectly. Studying SEM micrographs for pure $YBa_2Cu_3O_7$ that doped with AL_2O_3 with difference magnification (2μm, 50μm, 10μm, 5μm, 20μm), results images are found to have uniform and homogeneous distribution, and the effect of the doping of aluminum oxide to the composite samples decreases the grains of the image of the distortion in the shape and structure. Transmittance decreases with the increasing wavelength in the range (200- 300) nm, and then remains constant with increasing the wavelength, and absorbance increases with the increasing wavelength in the range (200- 300) nm, and then remains constant with increasing the wavelength. We Conclude that the optical constant of pure $YBa_2Cu_3O_7$ and $YBa_2Cu_3O_7$ which doped with AL_2O_3 increase with increasing energy of photon. We found the optical energy gap decrease when we increase the doping with $YBa_2Cu_3O_7$ which doped with AL_2O_3, and we found that the value of the energy gap is located between (8.56-4.39) EV. The decrease in optical energy gap lead to rise the value of the conductivity which can be useful in the developing of the solar cells. The optical conductivity increase with elevated of absorbance and when we use pure $YBa_2Cu_3O_7$ the absorbance elevated to high point at λ=202 nm with small grading in values and we doped $YBa_2Cu_3O_7$ with $AL_2O_{3\ also}$ the absorbance elevated with large grading in values and meet with pure $YBa_2Cu_3O_7$ in high value of absorbance at λ=202 nm which mean that the $YBa_2Cu_3O_7$ work perfectly at ultra violet area in the electromagnetic spectrum. We also subjected our sample for IV characterization at different sample at room temperature via

four-probe method and able to find the critical current density at the subsequent temperatures and found a decrement of critical current density with increment of temperature. We Conclude that The electrical conductivity for pure $YBa_2Cu_3O_7$ and $YBa_2Cu_3O_7$ doped with AL_2O_3 increase when increased the doping concentration.

4.5 Future work:

- Manufacturing the YBCO superconducting wires.
- Comparison between the mechanical properties and morphology structure (using SEM) of bulk and thin films of YBCO superconductors.
- Used the sputtering technique or pulsed laser deposition technique to prepare YBCO thin films.
- Preparing polymer-superconductor composite by using another polymer to study the structural , electrical and mechanical properties.

References:

[1] Hiroshi Kamimura, Hideki Ushio, ShunichiMatsuno, Tsuyoshi Hamada,(2005),Theory of Copper Oxide Superconductors, Berlin Heidelberg New York, 10 3-540-25189-8.

[2] AdirMoysesLuiz, (2010), Superconductor, JanezaTrdine, 51000 Rijeka, Croatia, ISBN 978-953-307-107-7 (chap3).

[3] Roland Hott, Reinhold Kleiner, Thomas Wolf& Gertrud Zwicknagl, (2004), SUPERCONDUCTING MATERIALS – A TOPICAL OVERVIEW, A. Narlikar (Ed.),“Frontiers in Superconducting

Materials",Verlag Berlin.

[4] NikolayPlakida,(2005),Theory of copper oxide superconductors,Verlag Berlin Heidelberg Germany, 978-3-642-12632-1.

[5]] C. U. Jung, J. Y. Kim, S. M. Lee, M.-S. Kim, Y. Yao, S. Y. Lee, S.-I. Lee, D. H. Ha Physica C 364-365 (2001) 225.

[6] P.J. (Peter John), (2004), The rise of the superconductors, Springer Printed in the United States of America, 0-7484-0772-3.

[7] Lawrence Dresner,(2002), Stability of Superconductors, ©2002 Kluwer Academic Publishers New York, Boston, Dordrecht, London, Moscow, 0-306-45030-5.

[8] T. Kawashima, Y. Matsui, E. Takayama-Muromachi, Physica C 254 (1995) 131.

[9] Bozovic, I., Logvenov, G., Belca, I., Narimbetov, B., & Sveklo, I. (2002). Epitaxial Strain and Superconductivity in L a 2− x S r x C u O 4 Thin Films. Physical review letters, 89(10), 107001.

[10] Naito, M., Karimoto, S., & Tsukada, A. (2002). Epitaxy-stabilized n-type superconducting cuprates. Superconductor Science and Technology, 15(12), 1663 35.

[11] Naito, M., & Hepp, M. (2000). Superconducting T′-La2-xCexCuO4 films grown by molecular beam epitaxy. Japanese Journal of Applied Physics, 39(6A), L485.

[12] Alff, L., Meyer, S., Kleefisch, S., Schoop, U., Marx, A., Sato, H., ... & Gross, R. (1999). Anomalous Low Temperature Behavior of

Superconducting Nd 1.85 Ce 0.15 CuO 4− y3037. Physical review letters, 83(13), 2644.

[13] Jin, C. Q., Yao, Y. S., Liu, S. C., Zhou, W. L., & Wang, W. K. (1993). Superconductivity and microstructure of n- type Ln1. 85Ce0. 15CuO4− y (Ln= Pr, Sm, Eu) produced under high pressure sintering. Applied physics letters, 62(23), 3037-3039.

[14] Iyo, A., Tanaka, Y., Tokumoto, M., & Ihara, H. (2001). High-pressure synthesis and properties of Ba2Can− 1CunO2n (O, F) 2 (n= 2–5) superconductors. Physica C: Superconductivity, 366(1), 43-50.

[15] A. R. West, (1974). Solid State Chemistry and Its Applications, Wiley, New York.

[16] H. Jensen, J. H. Pedersen, J. E. Jorgensen, J. Skov Pedersen,K.D Joensen, S.B. Iversen, E.G. Sogaard, (2006) J. of ExperiementalNanoscience, 1:355.

[17] Guanhua Chen ,Jean –Marc Langlois ,YuejinGuo and William GoddadrdIII,(1989) Superconducting properties of copper oxide high-temperature superconductors (YBaCuO/LaSrCuO/magnon pairing/generalized valence bond calculations/Heisenberg coupling term), Vol. 86, pp. 3447-3451, Chemistry.

[18] Hitoshi Oyama,TsuyoshiShinzato, Kazuhiko Hayashi, Kenji Kitajima,(2008). Application of Superconductors for Automobiles,Tsuyoshi ARIYOSHI and T akanoriSawalSei Technical Review · Number 67 . 36.

[19] Harshman, D. R., Fiory, A. T., & Dow, J. D. (2011). Theory of high-TC superconductivity: transition temperature.Journal of Physics: Condensed

Matter, 23(29), 295701.

[20] Peczkowski, P., Szterner, P., Jaegermann, Z., Kowalik, M., Zalecki, R., & Woch, W. M. (2018). Effects of Forming Pressure on Physicochemical Properties of YBCO Ceramics. Journal of Superconductivity and Novel Magnetism, 31(9), 2719-2732.

[21] Szterner, P., Pęczkowski, P., & Jaegermann, Z. (2017). Ceramiczne nadprzewodniki wysokotemperaturowe–otrzymywanie YBa2Cu3O7-x metodami prażenia. Prace Instytutu Ceramiki i Materiałów Budowlanych, 10.

[22] Howe, B. A. (2014). Crystal structure and superconductivity of YBa2Cu3O7-x.

[23] Giorgio Montaudo and Robert Lattimer, (2002), Mass spectrometry of polymer /, [24] ISBN 0-8493-3127-7. by CRC Press LLC. Budde W.L.analyical mass spectrometry, (2001), ACS andoxford University press wachington D.C and oxford.

[25] Kostjuk, S.V, Radchenko A.V , (2007), Ganachaud, F.Marcromolecules.

[26] Steffen M. Weidner† and Sarah Trimpin, (2008).Mass spectrometry of synthetic polymers, american chemical society,vol80,4349-4361.

[27] Scott D. Hanton, january (2004), New mass spectrometry techniques for the analysis of polymer for coatings applications, 7201 hamilton blvd,PA18195,VOI:610.481.8036.

[28] Edmond de Hoffmann and Vincent stoobant, (2007), Mass spectrometry (principles and applications), third edition,ISBN978-0-470-03310-4.